Environmental Earth Sciences (2023) 82:342
https://doi.org/10.1007/s12665-023-11024-9

ORIGINAL ARTICLE

Physical and mechanical properties of Ignimbrite from Arucas, Canary Islands

J. A. Valido[1] · J. M. Cáceres[1] · Luís M. O. Sousa[2]

Received: 31 March 2023 / Accepted: 8 June 2023 / Published online: 27 June 2023

Abstract

This research is a contribution to the mineralogical and physical–mechanical characterisation of the ignimbrites from Arucas (Gran Canaria Island), used as building stones under the commercial names of "Piedra de Arucas Lomo Tomás de León" and "Piedra de Arucas Rosa Silva". This stone has been used for more than five hundred years and is part of the local architectural heritage, but has also been exported to other regions of the world. To perform this characterisation, a chemical analysis was carried out using X-ray fluorescence (XRF), mineralogical and petrographic properties were obtained using polarised optical microscopy (POM), X-ray diffraction (XRD) and scanning electron microscopy (SEM). Several physical properties were determined, namely: apparent density (AP), open porosity (OP), water absorption at atmospheric pressure (WA), water absorption by capillarity (WAC), ultrasound velocity (PWV) and colour. Mechanical properties were obtained through compressive strength (UCS), bending strength (BS), point load (PLT), indirect tensile (BTS) and energy at break (IR) tests. To evaluate the durability, the samples were subjected to salt crystallisation cycles (CS), SO_2 action (AS) and salt spray (SS) and the abrasion resistance (AR) was determined. The results obtained show that, although both samples share the same lithology and belong to the same geological formation (Salic Formation, trachytic-phonolitic), they show very different properties. Porosity stands out as the property with the higher difference among the two studied varieties. Therefore, the application of these ignimbrites should be done accordingly, avoiding environmental conditions that promotes the wettability and/or the salt crystallisation.

Keywords Canary Islands · Building stone · Ignimbrite · Physical–mechanical properties · Durability

Introduction

Since ancient times, dimensional stones have been used as a material for building infrastructure, buildings of worship and monuments, many of which have become part of the cultural heritage in regions around the world (Seymour et al. 2004). Even the stones themselves, depending on their relevance throughout history can be considered as world heritage stone resources. Some examples are the granite of "Alpedrete" from Madrid (Freire-Lista et al. 2015a) and "Rosa Beta" from Italy (Careddu and Grillo 2015), the limestone "Lower Globigerina" from Malta (Cassar et al. 2017), or the "Marble" from Tennessee (Byerly and Knowles 2017). According to Cárdenes et al. (2022), the two ignimbrite objects of this study could be candidates for World Heritage status due to their undoubted value and importance in the development of the region and their use in singular works, dating back to the fifteenth century.

Knowledge of the petrographic, mineralogical and physico-mechanical properties of natural stones are essential, both to evaluate the most appropriate extraction systems of this resource in areas of exploitation (Carvalho et al. 2013; Sousa et al. 2016; Santos et al. 2018; Yarahmadi et al. 2019; Bogdanowitsch et al. 2022) and to assess the suitability of its use as dimension stone in modern buildings and in the restoration and conservation of architectural heritage (Siegesmund et al. 2018, Sousa et al. 2019, Freire-Lista et al. 2021, Ahmed et al. 2021).

✉ J. A. Valido
jvalidog@ull.es

[1] Department of Industrial Engineering, Escuela Superior de Ingeniería y Tecnología, Universidad de La Laguna, Campus Anchieta, 38200 La Laguna, Tenerife), Spain

[2] Department of Geology, University of Trás-Os-Montes e Alto Douro (Portugal); Geosciences Center, University of Coimbra, Coimbra, Portugal

The research carried out with the aim of characterising these materials is numerous and is reflected in the available literature. The following is a representative sample of them. Silva et al. (2010) performed a petrographic, mineralogical and physical-mechanical characterisation of basalts from the Azores (Portugal) and Alves et al. (2017) carried out a similar study with basalts from Madeira (Portugal). Granite has been extensively studied, Sousa et al. (2005) and Sousa (2014) did a comprehensive study of the physical–mechanical and durability properties of nine granites from NE Portugal used in the dimension stone industry. Freire-Lista et al. (2015b, 2016) studied the micro-fracturing induced by different accelerated ageing mechanisms of four granites from the Sierra de Guadarrama (Spain) and Mota-López et al. (2022) did an analytical characterisation of the granites used in the Roman amphitheatre of Emerita Augusta (present-day Mérida, Spain). Spathis et al. (2021) characterise the limestone from the archaeological site of Pella (Greece), Sousa et al. (2021) obtained the petrophysical properties of eleven sandstones from Portugal to study their behaviour under different environmental conditions and Merico et al. (2022) compare the limestone used in ancient times in the construction of the rural house in the Apulia region (Italy) with the limestone used today in its restoration.

Primavori and Angheben (2020) focus their research on porphyry "Trentino" from Italy, while Valido et al. (2021) characterise three porphyry varieties from China, and compare some of their properties with porphyry from other regions. Vavro et al. (2016) obtained the physical, mechanical and durability properties of Godula sandstones (Poland) and Ajanaf et al. (2020) studied sandstones from an ancient Roman settlement in NW Morocco. Navarro et al. (2017) characterises the main types of marble extracted in the Macael region (Almeria, southeastern Spain) and Lezzerini et al. (2021) determined the chemical, mineralogical and petrographical characteristics, as well as the main physical and mechanical properties of marble from Tuscany (Italy), coming from two inactive quarries.

These articles represent some of the recent research performed for a particular type of stone (basalts, granites, porphyries, sandstones, etc.). They are a clear example of the interest that the scientific community has always shown in knowing the petrographic, mineralogical, physical–mechanical and durability properties of building stone, either because they have been used in the past, are being used in the present or because they are likely to be used in the future. Although not cited in this work, other types of stone, have also been the object of study such as travertine, gneiss or schist.

Historically, ignimbrites have been of the one of the most widely used types of volcanic stone as a building material. This is due to their characteristics; colour, lightness and good insulating properties, and mainly their ease of workability (Heiken 2006), making ignimbrites a type of stone extensively studied. Wedekind et al. (2011) studied the effects of weathering on a group of tuffs and ignimbrites used in three historic buildings in Mexico City. With a similar aim, López-Doncel et al. (2013) analysed the petrographic, petrophysical, mineralogical and geochemical properties of a tuff quarried in central Mexico. Wedekind et al. (2013) investigated the deterioration caused by moisture expansion in tuffs from Mexico (including the above), Germany and Hungary. Tuffs from Mexico continue to be studied by López—Doncel et al. (2016, 2018) in relation to the deterioration produced by salt crystallisation and thermal expansion. Toprak and Arslanbaba (2016) studied the possibility of using tuff from Kütahya (Turkey) as a building stone and Yavuz et al. (2015) investigated the differences between tuff used as building stone in historical and modern buildings in western Turkey. Barbero-Barrera et al. (2019) determined the thermal and physical–mechanical properties of two tuffs from Gran Canaria (Spain) for use in the restoration of historic buildings. Koralay & Çelik (2019) characterise the Uşak ignimbrite (SW Turkey) and Bustamante et al. (2021) derive the properties of a group of ignimbrites used in the historical centre of Arequipa (Peru). In recently published research, Siegesmund et al. (2022) investigated and analysed a large group of tuffs from different states of Mexico used in building heritage sites. Pötzl et al. (2022) studied the petrography and petrophysics of a group of ignimbrites from Armenia, Germany and Mexico and carries out a correlation analysis including the properties of other ignimbrites from other regions and available in the literature. Finally, the study by Valido et al. (2023) regarding the physical properties, and the analyses of the degree of correlation between them, of four different ignimbrites according to their colour, extracted on the island of Tenerife (Spain), since together with the two ignimbrites included in present work are the most commonly used building stones in Canary Islands region.

The main objective of this study is the determination of the mineralogical, petrographic, petrophysical, mechanical and durability properties of the "*Piedra de Arucas*". The importance of characterising this stone lies in the fact that the "*Piedra de Arucas*" is widely used in modern architecture as a building stone, and it is present in some emblematic and important buildings and monuments, many of which have become part of the architectural heritage. This stone has been quarried for five centuries, and at present is extracted from two different quarries, and this research aims to make a comparison between these two varieties. The tests carried out provide the necessary data to evaluate the "*Piedra de Arucas*" as a building stone and to highlight the most notable differences depending on the quarry of origin. Moreover, given the importance of this stone from a heritage point of view, durability tests are a remarkable contribution to evaluating its resistance to deterioration, and therefore, provide

relevant information for the conservation and restoration of buildings and monuments where this stone is present.

Geological background

The Canary Islands is an archipelago of volcanic origin located in the Atlantic Ocean, in zone 28R according to the UTM (Universal Transverse Mercator) geographical coordinate system (Fig. 1), being one of the five archipelagos that make up the Macaronesian region. Gran Canaria is one of the seven islands from the Canary archipelago with its own administration, being, the second most populated. It rises 1958 m above mean sea level (*Morrón de La Agujereada*) and has a surface area of 1560 km^2, making it the third largest island after Tenerife and Fuerteventura.

The formation and geological evolution of the Canary Islands is still under debate and has given rise to different hypotheses; the propagating fracture, the uplift of tectonic blocks, the local Canary Islands rift, the blob model, etc. (Anguita & Hernán 2000). The most widely accepted hypothesis for its genesis is that its magmatism is associated with a hot spot related to the upwelling of an upper mantle plume (Holik et al. 1991; Carracedo et al. 1998; Negredo et al. 2022). As far as the island of Gran Canaria is concerned, and apart from the submarine construction phase (> 14.5 Ma) for which there is hardly any information, different magmatic phases of sub-aerial formation can be distinguished, which have been the subject of study in numerous investigations since the 1970s (Schmincke 1967, Feraud et al. 1981, Perez-Torrado et al. 1995, Carracedo et al. 2002, Van Den Bogaard 2013).

Shield construction is estimated to occur between 14.5—14.0 Ma (Van den Bogaard and Schmincke 1998). Some authors suggest that the shield was formed from several shield volcanoes (Schmincke 1993; Schmincke and Sumita 1998), others, consider the existence of a single shield volcano (Troll et al. 2002; Balcells et al. 1992). The volcanic eruptions of this stage are effusive in nature and gave rise to a large number of basic flows (> 1000 km^3) with few pyroclastic intercalations. This phase in which the shield volcanic edifice is built up is referred to by Balcells et al. (1992) as the Basaltic Formation (Fig. 2a). The speed at which the basalts and trachybasalts were emitted during this phase, together with the first ignimbritic eruptions, led to the emptying of the magma chamber and consequent collapse of the substratum of the shield volcano, causing the formation of the Tejeda caldera. (Fúster et al. 1968; Freundt and Schmincke 1995; Schmincke 1990).

With the formation of the Tejeda caldera begins a new stage of magmatism called the alkaline decay phase. This phase is characterised, in the first place, by the emission of differentiated felsic magmas of explosive character, mainly lavas and ignimbrites of trachytic-rhyolitic compositions (Fig. 2b) (14.0–13.3 Ma, volume estimates of about 300–500 km^3) and trachytic-phonolitic (Fig. 2c) (13.3–8.3 Ma, volume estimates > 500 km^3) (Carracedo et al. 2002), and secondly, by intrusions of alkaline syenites, phonolitic-nephelinite domes and the cone sheets system (12.3–7.3 Ma) (Fig. 2d) (Schirnick et al. 1999). These volcanic and subvolcanic materials are referred in the literature as being differentiated in a number of ways. For example, Fúster et al. (1968) divides them into two groups, the Trachy-Syenitic Complex and the Phonolitic Series, while Schmincke (1990) associates them with three formations; Tejeda, Mogán and Fataga. Continuing with the same criteria as in the previous phase, we will refer to the materials issued during this period as "Salic Formations", as proposed by Balcells et al. (1992).

After the shield formation phase and the alkaline decay phase, the island enters a period of volcanic dormancy (7.3–5.3 Ma). The sediments originating from this erosive period form alluvial deposits that constitute the "Lower Member of the Detritic Formation of Las Palmas" (FDLP) (Carracedo et al. 2002).

Volcanic activity is reactivated with Strombolian eruptions in the south and centre of the island. Subsequently, the magmatic activity moves towards the central zone giving rise to the formation of a stratovolcano "Roque Nublo" (Perez-Torrado et al. 1995). At first, the eruptions of this stratovolcano are effusive, emitting lavas of basanitic composition and alkaline basalts, but as the magma evolves into trachytic-phonolitic the eruptions become more explosive. This first phase of volcanic reactivation (5.3–3.0 Ma, volume estimates 200 km^3) (Carracedo et al. 2002) is referred to by Balcells et al. (1992) as the "Roque Nublo Cycle" (Fig. 2e). During this period, and at the same time as the volcanic activity of this first phase took place, marine sediments were deposited in the coastal area, forming the "Middle Member of the Detritic Formation of Las Palmas" and also developing an intense erosive activity on

Fig. 1 Location of the Canary Islands

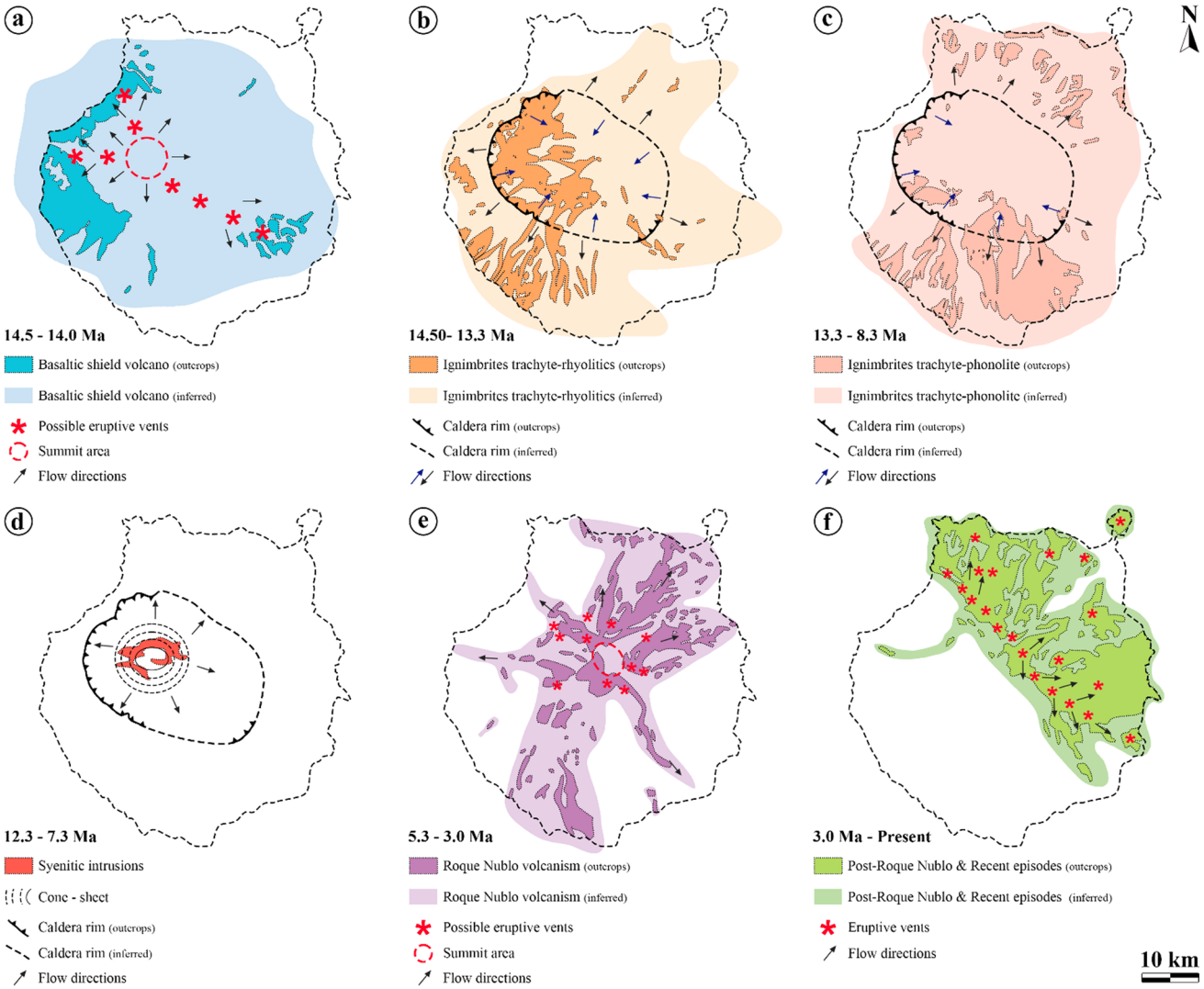

Fig. 2 Distribution of volcanism on the island of Gran Canaria (**a**) Basaltic formation, (**b**) Salic formations (Trachyte-rhyolitic), (**c**) Salic formations (Trachyte-phonolitic), (**d**) Salic formations (Syenite intrusions—Cone sheet), (**e**) Roque Nublo cycle and (**f**) Post Roque Nublo & Recent episodes cycle (modified from Balcells et al. 1992 and Socorro et al. 2005)

the volcanic materials that were being deposited, giving rise to the "Upper Member of the Detritic Formation of Las Palmas" (Cabrera 1985; Gabaldón et al. 1989).

Volcanic activity continues in a second phase (3.0–1.7 Ma, volume estimates > 30 km^3) although it is located exclusively in the northern half of the island (Machín 2009). This period is characterised by the emission of basanitic-nephelinitic to trachybasaltic lavas in Strombolian eruptions associated with a NW–SE oriented rift-like structure (Carracedo et al. 2002). This second phase within the volcanic reactivation, together with the most recent activity (1.7 Ma—present), typical of a very advanced post-erosive stage, is referred to by Balcells et al. (1992) as the "Post-Roque Nublo cycle and recent episodes" (Fig. 2f).

Materials and methods

Materials

The object of this study are two ignimbrites of trachytic-phonolitic composition, belonging to the extra caldera "Salic Formations", which occurred during the Miocene (13.3–8.3 Ma) (Fig. 2c). The material emitted during this stage covered a large area of Gran Canaria Island and gave rise to different geological units. The ignimbrites studied are extracted from the geological unit called "Arucas ignimbritic breccia" which outcrops in the north of the island (Fig. 3). This grey-bluish brecciated deposit is of the "block and ash" type, has a high degree of coherence

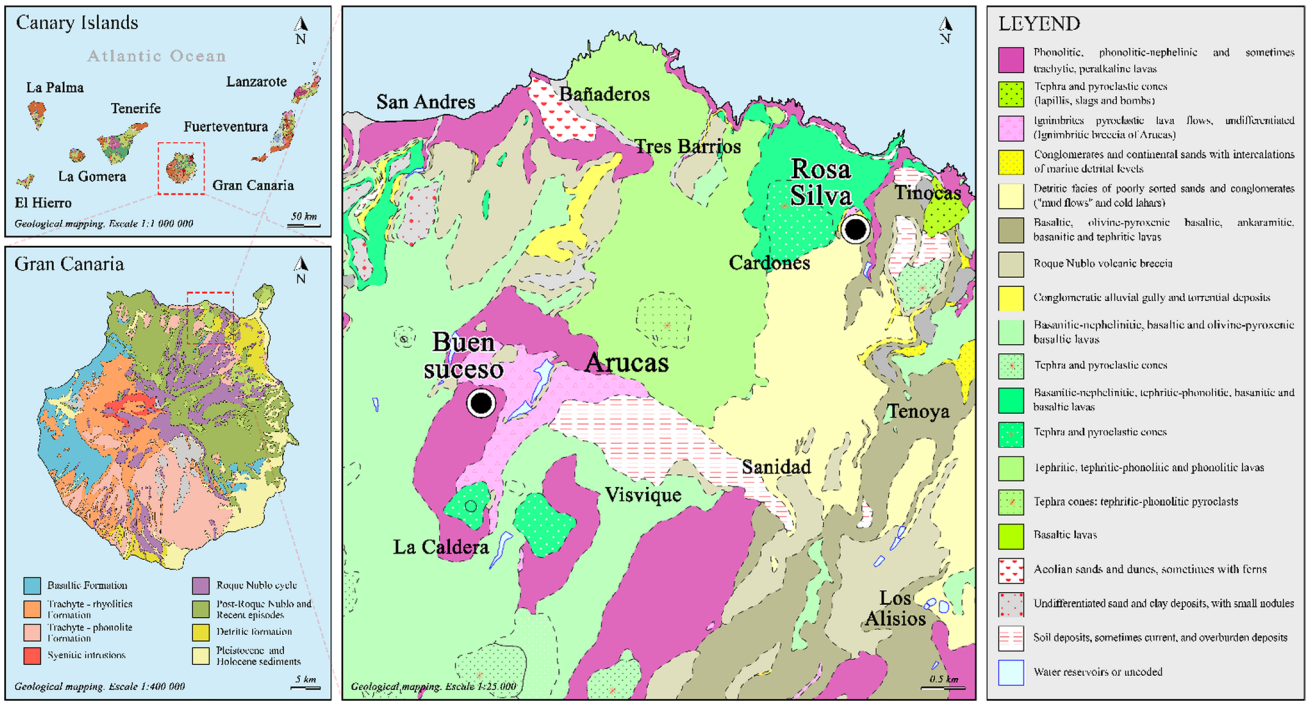

Fig. 3 Geological map with the distribution of the different geological units, the location of the quarry "Rosa Silva" and "Buen Suceso" and the population centres (modified from Balcells et al. 1992 and IGME 2021)

and consolidation, and normally occurs at a depth of 30 m, although it can sometimes reach up to 60 m.

One of the main and best-known outcrops of this breccia deposit is located in the municipality of Arucas. In the middle of the last century, more than thirty quarries were exploited in this area (Guillén 2006), mostly for the purpose of extracting from this ignimbritic deposit the stone known locally as "Piedra de Arucas", which, depending on its colour, could be distinguished between the "*Piedra Azul de Arucas*" (bluish) and the "*Piedra Gris de Arucas*" (greyish). From these quarries came the stones for the construction of the Templo Parroquial San Juan Bautista (Cathedral of Arucas), some of the buildings in the historic centre of the city of Las Palmas, such as the "*La Unión y El Fénix*" building, the Bank of Spain or the " Santa Catalina Hotel" and for the construction of the Cathedral Basilica of Santa Ana (a Site of Cultural Interest). This stone has also been used in the construction of buildings on other islands, such as the Cathedral of La Laguna or the General Captaincy of the Canary Islands in Tenerife (Balcells et al. 1992) (Fig. 4a–e). It was even exported to the "New World", as it came to be used as ballast on ships during the eighteenth century. There is evidence of its presence in southern Bolivia, in Venezuela (Canary Islands square of Caracas), in Havana (Cuba) and even in San Antonio, Texas (United States) (Marrero-Cabrera 2000).

The quarries located within the town centre have disappeared as a result of urban growth, with the exception of the "*El Cerrillo*" quarry, which has been converted into a museum ("*La Cantera*" Museum). This museum, the "*Centro de Interpretación del Labrante*" and the sculptural ensemble "*Homenaje a Los Labrantes*" are evidence of the importance that the "*Piedra de Arucas*" and its workers have had in the urban and socio-economic development of this municipality. And although the rest of the historical quarries are abandoned or have limited extraction, the "*Piedra de Arucas*" is still used as a building stone in modern architecture (Fig. 4f–n) thanks to two quarries still active today.

The extraction and marketing of this stone is carried out by the company "*Cantería de Arucas S.L.*" under the trade names of "*Piedra de Arucas Rosa Silva*" (RS) and "*Piedra de Arucas Lomo Tomás de León*" (LT). These ignimbrites are traded under the name of "*Piedra de Arucas*", but they are differentiated according to the quarry of origin, "*Rosa Silva*", or the place of extraction, "*Lomo Tomás de León*" (quarry "*Buen suceso*") (Fig. 3 and 5).

Methods

The laboratory tests used to characterise the ignimbrites in this work have been divided into four groups. Mineralogical and petrographic properties have been determined by chemical analysis using X-ray fluorescence, petrographic analysis,

Fig. 4 Examples of buildings and monuments with "Piedra de Arucas". **a** Templo Parroquial San Juan Bautista—Arucas, **b** National Spanish Bank—Las Palmas, (c) Captaincy General of the Canary Islands—Santa Cruz de Tenerife, (d) La Laguna Cathedral—San Cristóbal de La Laguna, (e) Santa Ana Cathedral—as Palmas, (f) Villa del Conde Hotel—Maspalomas, (g) Bench – Valsequillo, (h) Sculpture in private house—Madrid, (i) Private house—Ingenio, (j) Water fountain in tourist office—Arucas, (k) Water sheet in lawyer's office—Vegueta (Las Palmas), (m) Pedestrian street—Arucas and (n) Private house—Dublin (Irland) (f-n courtesy of Canteria Aruccas S.L.)

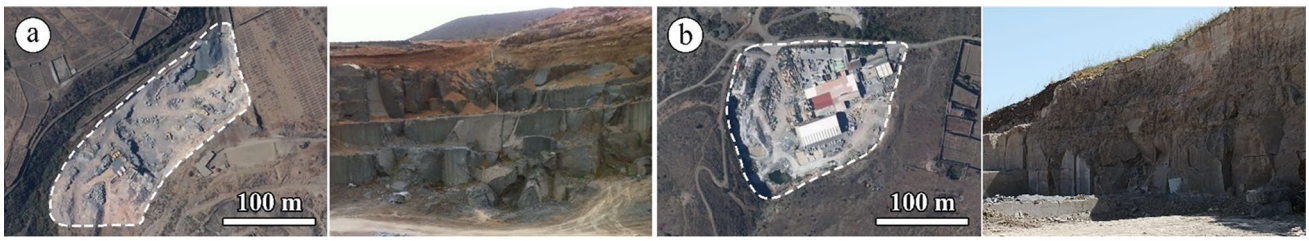

Fig. 5 Location of the (a) quarry "Rosa Silva" (28º08′18.95'' N—15º29′54.85'' W) and (b) quarry "Buen Suceso" and extraction company "Cantería de Arucas S.L" (28º07′10.26'' N—15º32′40.39'' W)

mineralogical analysis by X-ray diffraction and scanning electron microscopy. Petrophysical characterisation was carried out by measuring the following properties: apparent density, open porosity, water absorption at atmospheric pressure, water absorption coefficient by capillarity, ultrasound propagation velocity and colour. The mechanical properties

were determined by the following tests: uniaxial compression strength, flexural strength under concentrated load, point load resistance, indirect tensile strength and rupture energy. Finally, durability is assessed by means of: abrasion, salt crystallisation, ageing by salt mist and ageing by SO_2. All tests were carried out according to the guidelines and indications of the corresponding standards, following the described methodology and using the recommended dimensions and number of specimens. As it is set out in the standards, in all cases the tests were done once the specimens were dried to constant mass (weighing each 24 h until less than ± 0.1% variation in mass).

Mineralogical and petrographic properties

The chemical composition was obtained through chemical analysis by the X-Ray Fluorescence (XRF), as described in the UNE-EN 15309 standard (AENOR 2008b), and was carried out by the Activation Laboratories Ltd. (Canada), that has ISO/IEC 17025 and CAN-P-1579 accreditation for mineral analysis. For the petrographic analysis (POM—polarised optical microscopy), a thin section was examined, for each of the samples in order to identify the stone's minerals, texture and structure, in accordance with the UNE-EN 12407 standard (AENOR 2007a). For X-ray diffraction (XRD), the samples were previously pulverised to a particle size below 63 µm and a PANalytical X'Pert PRO MPD with X'Celerator detector and secondary monochromator was used. The scanning electron microscopy (SEM) analysis was carried out by Electronic Microscopy Unit of University of Trás-os-Montes e Alto Duero. A FEI Quanta 400 scanning electron microscope was used to obtain the SEM images.

Petrophysical properties

The apparent density (AP) and open porosity (OP) was evaluated based on UNE-EN 1936 standard (AENOR 2007b). Apparent density and open porosity were determined by vacuum absorption of water hydrostatic weighing. The water absorption at atmospheric pressure (WA) was determined according to the methodology described in UNE-EN 13755 standard (AENOR 2008b, a). The specimens are placed in a tank and water is added gradually until fully immersed. They are then weighed at 24 h intervals until they reach constant mass. The water absorption coefficient by capillary (WAC) was determined following the specifications described in the UNE-EN 1925 standard (AENOR 1990), parallel and perpendicular to the anisotropy planes. The specimens are placed on supports in a tank and water is added until the base of the specimens is partially submerged to a depth of 3 mm. Initially, the samples are weighed at different time intervals, then every 24 h until a constant mass is reached. If the graph obtained can be satisfactorily approximated by two straight lines and the regression coefficient obtained for the first section is greater than 0.90, the water absorption coefficient by capillary is the slope of this regression line. However, if this approximation is not possible, the absorption coefficient is determined by the fitting equation (Eq. 1), corresponding to the model proposed by Feng & Janssen (2018).

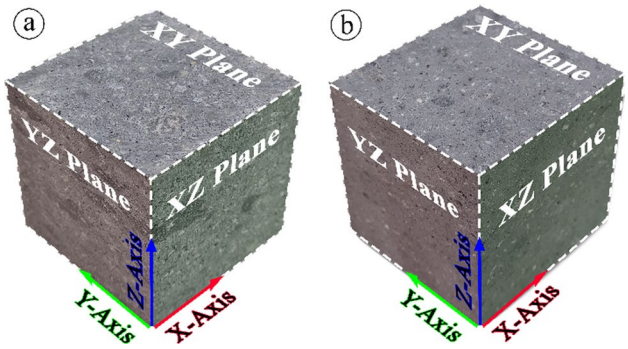

Fig. 6 Test direction (X, Y and Z) (**a**) RS and (**b**) LT

$$\frac{m_i - m_d}{A} = W_{ac} \cdot b \cdot \left(0.5103 - 1.3849 \cdot e^{-\frac{t_i}{b^2}-1}\right)^{0.3403} + c \quad (1)$$

where m_i is the wet mass (g) in the time (t_i); m_d is the dry mass (g); A is the submerged base area (m^2) and b and c are fitting parameters.

The test to determine the ultrasound P-wave velocity propagation is carried out according to UNE-EN 14579 standard (AENOR 2005). The propagation velocity is obtained as the ratio of the travel length to the time elapsed between the start of the pulse generated at the transmitting transducer and the detection of its arrival at the receiving transducer. The ultrasound velocity is measured in the three axis direction to calculate the anisotropy indexes (Eq. 2, 3) of (Guyader & Denis 1986).

Total anisotropy index (%):

$$\Delta M\% = 100 \times \left[1 - \frac{2V_{p_z}}{V_{p_x} + V_{p_y}}\right] \quad (2)$$

Relative anisotropy index (%) :

$$\Delta m\% = 100 \times \left[\frac{2\left(V_{p_x} - V_{p_y}\right)}{V_{p_x} + V_{p_y}}\right] \quad (3)$$

where V_{px} is the wave velocity in direction X-axis; V_{py} is the wave velocity in direction Y-axis and V_{pz} is the wave velocity in direction Z-axis (Fig. 6).

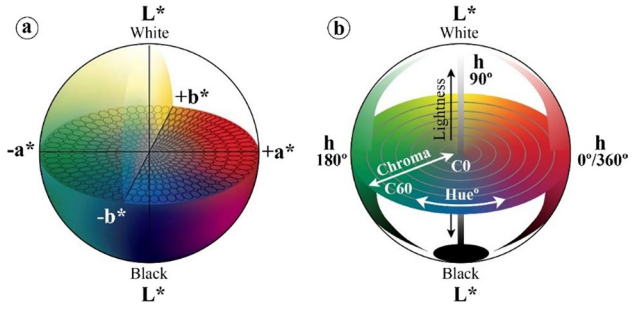

Fig. 7 Color space (**a**) CIELab model and (**b**) CIELCh model (modified from X-Rite)

Colour was assessed according to UNE-EN 15886 standard (AENOR 2011) and was determined using a X-Rite colorimeter (model 964), 0° viewing angle geometry and specular component included with D65 illuminant. Colour is expressed using CIELab (Fig. 7a) and CIELCh (Fig. 7b) systems. In the CIELab system, the colour is quantified according to three chromatic coordinates. The L* parameter represents lightness or luminosity (L* = 0 dark; L* = 100 white), and the a* parameter is the red–green axis (a* > 0 red; a* < 0 green) and the b*-parameter is the yellow–blue axis (b* > 0 yellow; b* < 0 blue). The attributes of the CIELCh systems are the chroma ($C^*_{ab} = (a^{*2} + b^{*2})^{1/2}$) and the hue ($h_{ab} = \tan^{-1} b^*/a^*$).

The colour difference between the two samples studied is obtained numerically as a function of the overall colour variation calculated according to Eq. (4). A value of ΔE* < 2 means that an observer will hardly be able to perceive the colour difference, while values of ΔE* between 2–3.5 mean that the colour difference between the two samples is more noticeable. A value of AE* > 5 means that the colours are perceived as two different colours (Mokrzycki & Tatol 2011).

Total colour difference:

$$\Delta E^* = \sqrt{(\Delta L^*)^2 + (\Delta a^*)^2 + (\Delta b^*)^2} \quad (4)$$

In order to carry out these tests, corresponding to obtaining the petrophysical properties, six cubic specimens with an edge of 50 mm per sample were taken for each one.

Mechanical properties

The uniaxial compressive strength (UCS) is determined according to the UNE-EN 1926 standard (AENOR 2007c). The specimens are placed between two steel plates and a load is applied at constant speed until failure occurs. Depending on the arrangement of the specimens, it is possible to perform this test in the Z-axis direction, when the load is applied perpendicular to the anisotropy planes, or in the X or Y-axis direction, when the load is applied parallel to the anisotropy planes. A total of twenty 50 mm edge cubes were tested (ten in the Z-axis direction and ten in the X-axis direction). The flexural strength under concentrated load (FS) is obtained according to UNE-EN 12372 standard (AENOR 2007a). The specimens are placed between two rollers and by means of a central roller a load is applied at a constant speed until breakage occurs. Depending on how the specimens are prepared, this test can be carried out in three different arrangements. In this case, the flexural strength was obtained by applying the load perpendicular to the anisotropy planes (in the direction of the Z-axis), as this is the arrangement that offers the highest strength and is generally used in the several utilizations. Ten specimens (180 × 60 × 30 mm) were tested. The point load strength (PLT) was determined according to ASTM D5731 standard (ASTM 2016b) in a diametral test configuration. The specimens are subjected to a concentrated load using a pair of spherically truncated conical punches until breakage occurs. Ten were core with a length/diameter ratio major to the unit were tested and the results were corrected to a specimen diameter of 50 mm. The splitting tensile strength test (STS) was carried out in accordance with the ASTM D3967 standard (ASTM 2016a) and determined by means of the "Brazilian test" used to indirectly determine the tensile strength. The specimens are placed between two jaws so that the axes of rotation of both (specimen and jaws) coincide and an axial load is applied until breakage occurs. Cylindrical specimens, 50 mm in diameter and 25 mm thick (disc type) were used. The cores used to determine the point load strength and the indirect tensile strength come from drilling a borehole in a block in a direction perpendicular to its plane of anisotropy. The rupture energy (RE) was determined according to the UNE-EN 14158 standard (AENOR 2004b). A steel ball of mass 1 kg is dropped onto the centre of the specimen which is placed on a bed of sand, and the height of the ball drop is gradually increased until the specimen breaks. Six specimens of dimensions (200 × 200 × 30 mm) were tested.

Durability assessment

Abrasion resistance (WWA) is obtained according to UNE EN 14157 standard (AENOR 2005a), using the wide wheel abrasion method. Each specimen is placed in contact with an abrasive disc while corundum is poured in as abrasive material. After 75 laps, the footprint is measured and its dimension is corrected by a calibration factor. The surface of the test specimens has been painted to facilitate the measurement of the footprint. Six specimens (100 × 100 × 20 mm) were tested. The resistance to salt crystallisation (SC) is determined according to UNE-EN 12370 standard (AENOR

2020). The test specimens are immersed in a 14% sodium sulfate decahydrate solution ($Na_2SO_4 \cdot 10\ H_2O$) for 2 h and then dried for 20 h in an oven at 100 °C. After cooling the test specimens to ambient temperature (2 h), they are again immersed in the solution. This process is repeated 15 times. Six cubic specimens (edges measuring 40 mm) were taken. To determine the resistance to ageing by salt mist (SM), the indications of the UNE-EN 14147 standard (AENOR 2004a) are followed. The specimens are placed inside a chamber at 35 °C and exposed to 60 cycles consisting of 4 h of salt spray (sodium chloride solution with a salt concentration of 100 ± 10 g/l) and 8 h of drying. Six cubic specimens were used (edges measuring 50 mm). The resistance to ageing by the SO_2 action in the presence of humidity (SO) is obtained according to UNE-EN 13919 standard (AENOR 2003). The number of specimens to be tested is divided into two equal groups. Each group is immersed for 21 days in a solution with a different concentration of sulphurous acid. Solution A has been prepared 150 ± 10 mL deionize water and 500 ± 10 mL H_2SO_3 acid. Other Solution B has been prepared 500 ± 10 mL deionize water and 150 ± 10 mL H_2SO_3 acid. Six specimens ($120 \times 60 \times 10$ mm) were tested. Resistance to salt crystallisation (SC), resistance to ageing by salt mist (SM) and resistance to ageing by SO_2 action are evaluated as a function of the mass variation of the specimens at the beginning and at the end of the test.

Results and discussions

As long as the results are quantitative, a table with average values, maximum, minimum and standard deviation will be displayed. Tests performed in more than one direction shall include the results for each direction, when this is not indicated, the direction tested is the one corresponding to the Z-axis (perpendicular to the anisotropy planes). The results are discussed and compared with those obtained in other studies, especially in those dealing with the same type of stone.

Table 1 Major element oxides chemical composition of ignimbrite samples

Chemical composition (wt %)	RS	LT
SiO_2	62.00	62.99
Al_2O_3	16.92	17.07
Fe_2O_3	4.07	4.19
MnO	0.23	0.21
MgO	0.94	0.46
CaO	0.76	0.45
Na_2O	6.66	6.36
K_2O	5.55	5.38
TiO_2	0.87	0.90
P_2O_5	0.12	0.05
LOI	2.06	1.94
Sum	100.20	99.99

Mineralogical and petrographic analyses

X-Ray Fluorescence (XRF)

The geochemical compositions of the ignimbrite samples are presented in Table 1. The "*Rosa Silva*" ignimbrite and the "*Lomo Tomás de León*" ignimbrite have a very similar chemical composition. The variation, in weight percentage of the compounds, is less than 0.5%, except for silicon dioxide (SiO_2), which is 1%. Silicon dioxide (SiO_2) and aluminium oxide (Al_2O_3) are the major chemical compounds. Sodium (Na_2O), potassium (K_2O) and iron (Fe_2O_3) oxides, each with a proportion between 5 and 7%, are the next highest components by weight. The rest appears in a proportion of less than 1%, so their content in the samples is insignificant. The Loss on Ignition (LOI) values are related to carbon dioxide (CO_2) (carbonate rocks, organic materials) and water (H_2O) (mica, amphiboles, clay minerals) contents.

Projecting the total weight percentages of alkalis ($Na_2O + K_2O$) and silica (SiO_2) on a TAS diagram (Bas et al. 1986) shows that both ignimbrites have a trachytic composition (Fig. 8a). In order to analyse the weathering of the samples, the chemical alteration index (CIA) defined by Nesbitt & Young (1982) is calculated according to Eq. 5.

Chemical Index of Alteration (CIA):

$$CIA = \frac{Al_2O_3}{Al_2O_3 + CaO^* + Na_2O + K_2O} \times 100 \quad (5)$$

Each oxide (Al_2O_3, CaO*, Na_2O, K_2O) is expressed in molar ratios. The CaO* ratio corresponds to the amount of CaO incorporated in the siliceous fraction of the sample and is obtained by applying the method proposed by McLennan (1982). The chemical alteration index (CIA) is based on the measurement of feldspar weathering, a process in which the proportion of Al_2O_3 increases over alkalis (CaO, Na_2O, K_2O). A value of CIA < 50 indicates that the rock is undisturbed; 50 < CIA < 60, slightly weathered; 60 < CIA < 80, moderately weathered; CIA > 80 heavily weathered. The CIA values obtained are 48 in the ignimbrite "*Rosa Silva*" and 50 in the ignimbrite "*Lomo Tomás de León*", so that, according to this index, both samples are practically unaltered. Weathering intensity is usually defined by the ternary A-CN-K diagram (Shao et al. 2012) (Fig. 8b).

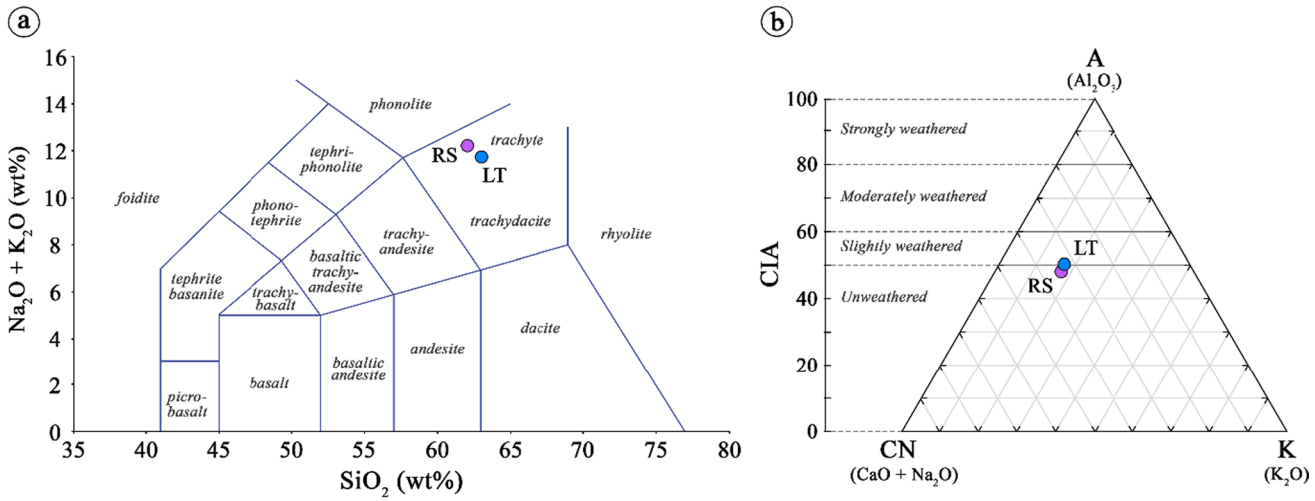

Fig. 8 Chemical classification: (**a**) Total Alkalis – Silica (TAS) Diagram and (**b**) A-CN-K ternary plot

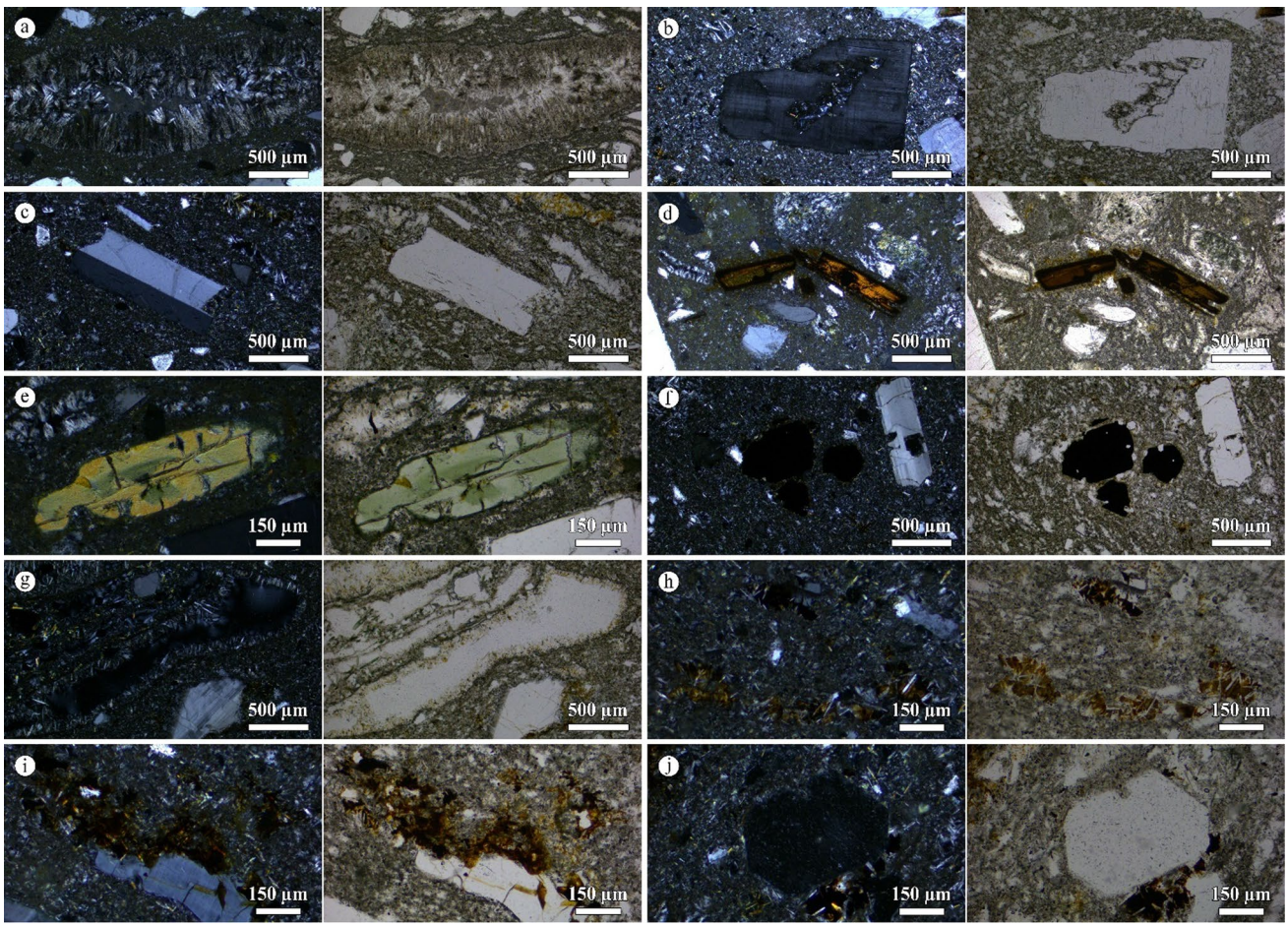

Fig. 9 Microphotographs with main minerals displayed (crossed polarized—left; plane polarized—right). **a** pumice fragments; **b** anorthoclase; **c** sanidine; **d** phlogopite; **e** augite; **f** opaques; **g** vesicle occupied by zeolites; **h**, **i** hydroxides and **j** pseudomorphosis of nepheline to sodalite

Polarised optical microscopy (POM)

Both the "*Rosa Silva*" ignimbrite and the "*Lomo Tomás de León*" ignimbrite correspond to an extrusive igneous rock, with an eutaxitic texture. It consists mainly of lithic and pumice fragments (both in high proportion) and phenocrysts contained in a cinereous matrix with vitreous characteristics. The lithic fragments are of phonolitic/trachytic composition, with a porphyritic texture and irregular shapes. The pumice fragments are elongated (flattened) with a banded appearance (fiammes) and are partially devitrified, forming fine needles of alkali feldspar and augite that are arranged radially or perpendicular to the fragment walls (Fig. 9a). The most abundant and also the largest phenocrysts are anorthoclase (Fig. 9b), oligoclase and sanidine (Fig. 9c). In smaller proportions, elongated tabular microphenocrysts of phlogopite (Fig. 9d) and augite (Fig. 9e) are present. Opaque minerals, possibly hematite, are also found sporadically (Fig. 9f). The vesicles are often occupied by zeolites, which are arranged radially around the cavity walls (Fig. 9g). The "*Lomo Tomás de León*" ignimbrite shows abundant iron hydroxides (Fig. 9h, i) as a consequence of a higher degree of alteration, and unlike the "*Rosa Silva*" ignimbrite, pseudomorphism of sodalite after nepheline is observed in this one, with generally hexagonal sections and always extinct (Fig. 9j), these being the most notable differences.

X-Ray diffraction (XRD)

The ignimbrites "*Rosa Silva*" and "*Lomo Tomás de León*" have a very similar mineralogical composition (Fig. 10). With different proportions for each of the two ignimbrites studied, the major minerals are anorthoclase, oligoclase and sanidine (the total modal proportion of these three minerals is over 90%). In the ignimbrite "*Rosa Silva*", anorthoclase predominates over oligoclase and sanidine, while in the "*Lomo Tomás de León*" ignimbrite it is oligoclase which is present in greater proportion, while sanidine and anorthoclase have similar proportions. The next most represented mineral is augite, followed by phlogopite, although the latter in a very low proportion. Sodalite and nepheline were only detected in the "*Lomo Tomás de León*" ignimbrite, as well as phillipsite, which only appears in the "*Rosa Silva*" ignimbrite.

Scanning electron microscopy (SEM)

Analysis of the scanning electron microscope images shows some significant differences in the distribution of the crystals and in the characteristics of the matrix containing them. The crystals of the ignimbrite "*Rosa Silva*" (Fig. 11a) are larger and more abundant than those of the ignimbrite "*Lomo Tomás de León*" (Fig. 11b). In the SEM image corresponding to the "*Rosa Silva*" ignimbrite, a cluster of crystals can be easily identified, while in the "*Lomo Tomás de León*" ignimbrite, what can be seen in greater proportion is the matrix surrounding a fragment of pumice. The matrix of the "*Rosa Silva*" ignimbrite is clearly denser, no pores are visible on the viewing scale. In the ignimbrite "*Lomo Tomás de León*", on the other hand, a less cohesive matrix can be observed and, on the contrary, pores can be identified in this ignimbrite.

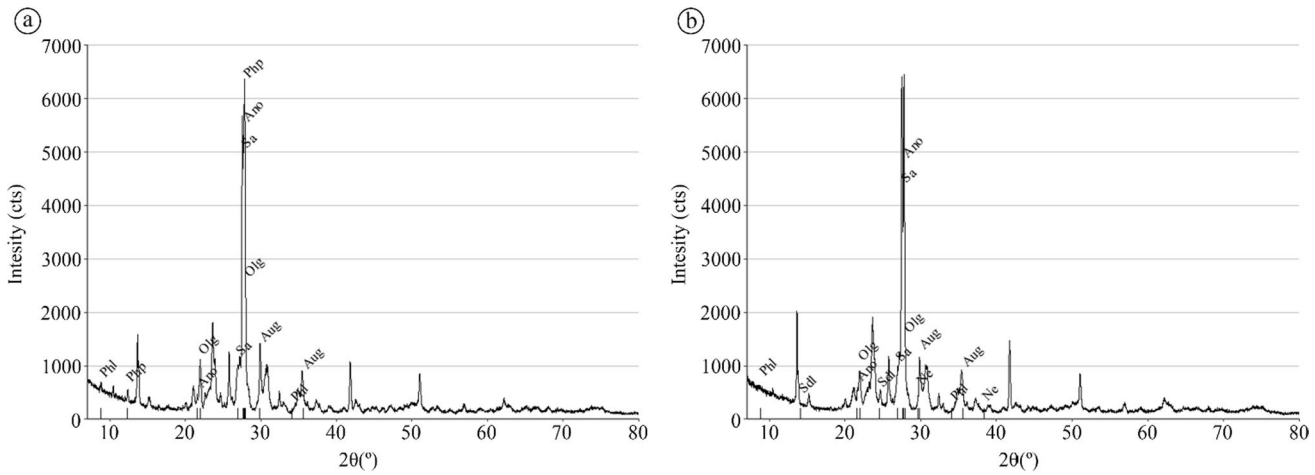

Fig. 10 Diffractograms. **a** RS and **b** LT. Minerals: Anorthoclase (Ano), Augite (Aug), Hematite (Hem), Nepheline (Ne), Oligoclase (Olg), Phillipsite (Php), Phlogopite (Phl), Sanidine (Sa), Sodalite (Sdl) (Warr 2021)

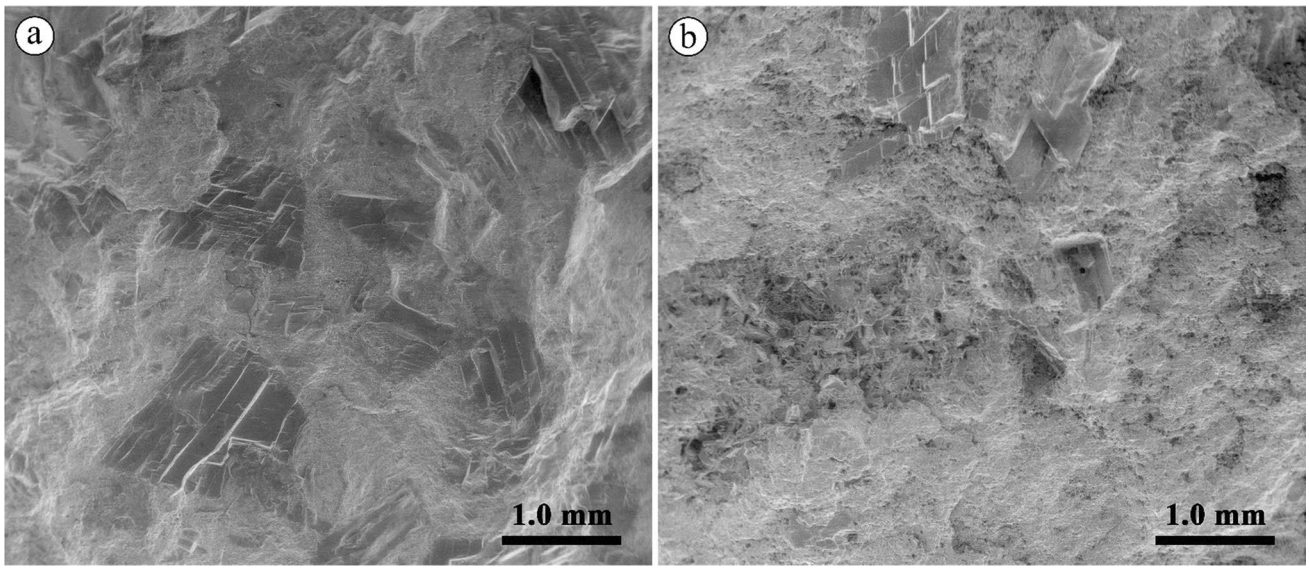

Fig. 11 SEM image **a** RS and **b** LT

Table 2 Results of apparent density (AD), open porosity (OP) and water absorption at atmospheric pressure (WA) test

Ignimbrite	AD (g/cm^3)				OP (%)				WA (%)			
	Max	Min	Mean	SD	Max	Min	Mean	SD	Max	Min	Mean	SD
RS	2.39	2.38	2.38	0.01	4.19	2.75	3.20	0.53	2.91	2.45	2.67	0.17
LT	2.12	2.05	2.09	0.03	18.71	16.96	17.63	0.79	7.84	6.65	7.30	0.40

RS: Rosa Silva; LT: Lomo Tomás de León

Petrophysical properties

Apparent density (AD) and open porosity (OP)

The ignimbrite "*Rosa Silva*" has a bulk density of 2.38 g/cm^3 and an open porosity of 3.20%, while the bulk density and open porosity of the "*Lomo Tomás de León*" ignimbrite are 2.09 g/cm^3 and 17.63%, respectively (Table 2). According to the classification proposed by Anon (1979), the "*Rosa Silva*" ignimbrite shows a medium density and the "*Lomo Tomás de León*" ignimbrite a low density. The difference in porosity between these two ignimbrites is more significant than the difference in density. In qualitative terms, and according to the classification of Anon (1979), the "*Rosa Silva*" ignimbrite has a very low porosity, while the porosity of the "*Lomo Tomás de León*" ignimbrite is high. The studied ignimbrites show density values similar to those reported in the literature, where the density ranges between 1.1 and 2.9 g/cm^3 (Engidasew 2014, Engidasew and Abay 2016, Yüksek and Demirci 2010, Kekec and Gokay 2009, Martínez-Martínez et al. 2018, Öner et al. 2006, Akın et al. 2017, Korkanç 2007, Özbek 2014). Similarly, the open porosity obtained is also within the expected for this lithotype, however, it should be noted that it is not common to find ignimbrites with porosity as low as that of the "*Rosa Silva*" ignimbrite. Some of the ignimbrites studied by Engidasew and Abay (2016) have porosities between 1.37 and 4.27%, as well as one of the varieties investigated by Valido et al. (2023) in which a porosity of 2.18% was obtained, however, the mean porosity for this lithotype is usually between 20 and 35% (Pötzl et al. 2022).

Water absorption at atmospheric pressure (WA)

The results of the water absorption test at atmospheric pressure are shown in Table 2. The water absorption at atmospheric pressure of the "*Rosa Silva*" ignimbrite is 2.67%, while the "*Lomo Tomás de León*" ignimbrite shows a water absorption of 7.30%. These results were to be expected, as the "*Lomo Tomás de León*" ignimbrite has a much higher porosity than the "*Rosa Silva*" ignimbrite (five times higher), which gives it a greater water absorption capacity. It is true that the difference is not as notable as in the porosity, but even so it means that the water absorption of the "*Lomo Tomás de León*" ignimbrite is practically double that of the "Rosa Silva" ignimbrite. According to literature data compiled by

Table 3 Results from water absorption coefficient by capillarity test

Ignimbrite		WAC ($g/m^2 \cdot s^{0.5}$)			
		Max	Min	Mean	SD
RS	*X*	1.86	1.18	1.44	0.28
	Z	1.91	1.44	1.70	0.18
LT	*X*	22.22	15.37	19.80	2.41
	Z	20.42	13.41	16.94	2.75

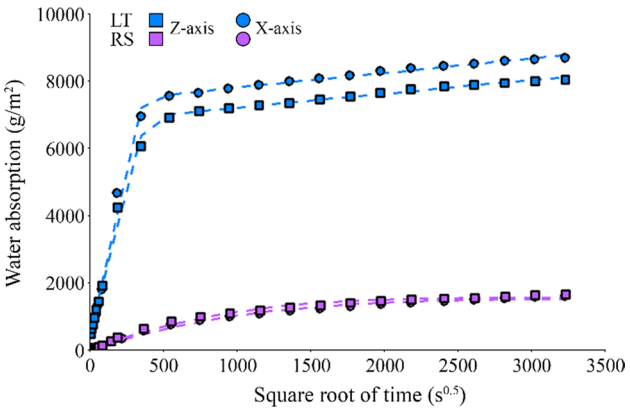

Fig. 12 Mass of water absorbed as a function of the square root of time

Pötzl et al. (2022), the water absorption at atmospheric pressure for this type of stone is usually between 10 and 20% (Özşen et al. 2017, Çelik & Ergül 2015; Ünal 2011; Akın et al. 2017). However, this lithology presents a great variability, being possible to find in the literature ignimbrites with water absorption close to 30% (Germinario and Török 2019, Bozdağ & İnce 2018, Sert & Özkahraman 2016, Bustamante et al. 2021) and even higher than 40% (López-Doncel et al. 2018) and others with absorptions lower than 5% (Engidasew and Abay 2016; Celik et al. 2020). The ignimbrites in this study have low water absorption, lower than the mean range estimated for this type of stone.

Water absorption coefficient by capillarity (WAC)

The capillary water absorption coefficient of the "*Rosa Silva*" ignimbrite is 1.44 $g/m^2 \cdot s^{0.5}$ and 1.70 $g/m^2 \cdot s^{0.5}$ depending on the test direction, X and Z, respectively. The ignimbrite "*Lomo Tomás de León*" has a higher absorption coefficient, 19.80 $g/m^2 \cdot s^{0.5}$, when the water rises parallel to the anisotropy planes (X-axis) and 16.94 $g/m^2 \cdot s^{0.5}$ when it rises perpendicularly (Z-axis) (Table 3). The values of capillary absorption in the two directions show small differences, close to 15% in both ignimbrites. The "*Lomo Tomás de León*" ignimbrite shows a slight tendency to a greater absorption parallel to the planes of weakness, whereas the opposite is true for the "*Rosa Silva*" ignimbrite. According to the classification proposed by Snethlage (2005), these two ignimbrites have a very low capillary water absorption capacity, < 8 $g/m^2 \cdot s^{0.5}$.

The "*Lomo Tomás de León*" ignimbrite, the typical capillary absorption curve was obtained, in which two straight sections are clearly identified, in this case, the capillary absorption coefficient corresponds to the slope of the regression line of the first section (Fig. 12). On the other hand, the curve obtained in the "*Rosa Silva*" ignimbrite cannot be approximated by two sections, so the capillary absorption coefficient corresponds to the value of W_{ac} of the fitting equation (Eq. 1). The dots correspond to the mean

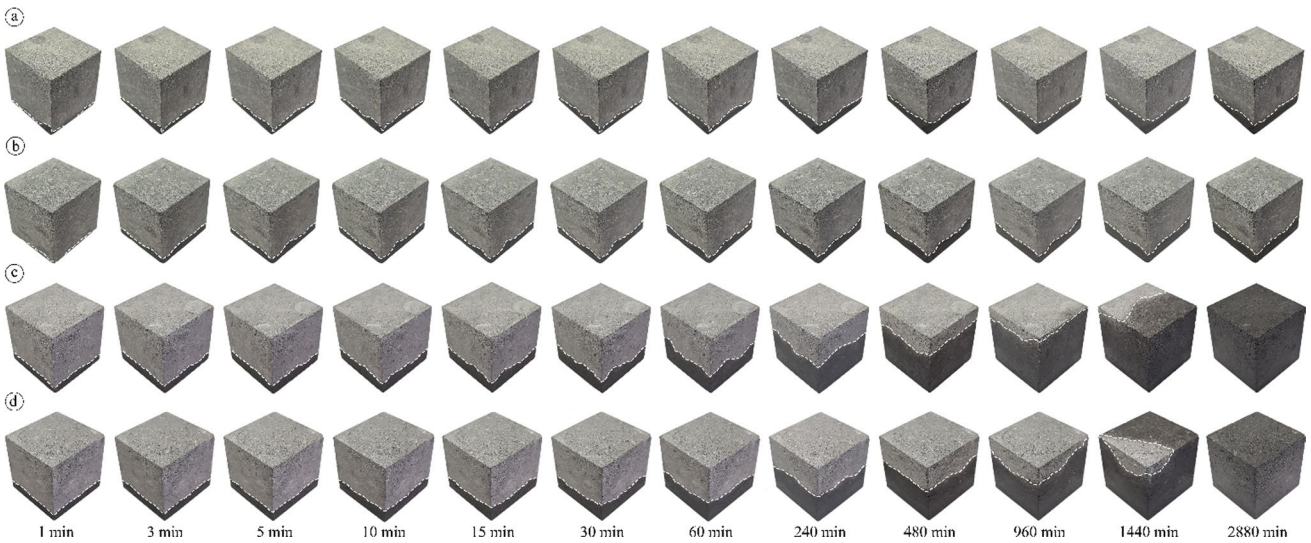

Fig. 13 Capillary water uptake over time **a**–**b** RS; **c**–**d** LT; **a**, **c** X-axis and **b**, **d** Z-axis

absorption values of the six specimens tested in each direction (X and Z). The dashed line represents the best fitting.

The water capillary absorption coefficient reported by other authors for this lithotype has a very wide range (0.70–850 g/m^2·s$^{0.5}$) (Martínez-Martínez et al. 2018, Cueto et al. 2018), with a mean value around 250 g/m^2·s$^{0.5}$ (Bustamante et al. 2021, Iucolano et al. 2019; Ünal and Altunok 2019). The capillary absorption coefficients of the ignimbrites "*Lomo Tomás de León*" and "*Rosa Silva*", lower than 20 g/m^2·s$^{0.5}$ in any case, are well below the mean value, which means that they are among the ignimbrites with the lowest absorption.

The level of water absorbed by capillary action (Fig. 13) reproduce the absorption coefficients obtained (Table 3). The level of water in the "*Rosa Silva*" ignimbrite is close to the base, remaining practically constant after 480 min, corroborating its low absorption capacity by capillary action (< 2.0 g/m^2·s$^{0.5}$). During the same period, the level of water absorbed in the "*Lomo Tomás de León*" ignimbrite, which has a much higher absorption coefficient (≈ 20 g/m^2·s$^{0.5}$), is in the upper half of the height of the test specimen, reaching full wetting after 48 h (2880 min). The difference in the level of water absorbed by capillary action between the two directions tested (X-axis and Z-axis) is not visually noticeable, coinciding with the small difference in the capillary absorption coefficients obtained between the two directions.

Ultrasound propagation velocity

Taking as ultrasound velocity the mean value of the velocities measured in each of the directions, it is observed that the wave was able to travel at a higher velocity in the "*Rosa Silva*" ignimbrite, with a velocity close to 5000 m/s, than in the "*Lomo Tomás de León*" ignimbrite, 4000 m/s. This difference in velocity is practically maintained in all three directions (Table 4). These results are coherent with the density and porosity values obtained, in which the "*Rosa Silva*" ignimbrite is denser and less porous than the "*Lomo Tomás de León*" ignimbrite, favouring the wave to travel at a higher velocity.

The ultrasound velocity in ignimbrites is highly variable, with values ranging from approximately 1200 m/s (Çelik and Aygün 2018) to 4900 m/s (Rodríguez-Losada et al. 2007). Apart from these values, which correspond to the extremes, the mean velocity of this lithology is close to 2500 m/s (Teymen and Mengüç 2020; Vanorio et al. 2002; Ünal 2011, Martínez-Martínez et al. 2018, Özşen et al. 2017) and both the "*Lomo Tomás de León*" ignimbrite and the "*Rosa Silva*" ignimbrite present ultrasound velocities that greatly exceed this value. In fact, the ultrasound velocity obtained in the "*Rosa Silva*" ignimbrite is even higher than the maximum propagation velocity found in the literature for this type of stone.

The anisotropy indices obtained are very low. The total anisotropy index (Eq. 2) of the "*Rosa Silva*" ignimbrite is 0.7% and of the "*Lomo Tomás de León*" ignimbrite, equal to its relative anisotropy, 2.2%. The relative anisotropy index (Eq. 3) of the "*Rosa Silva*" ignimbrite is even lower, 0.06%. From the anisotropy indices obtained, it can be concluded that the samples are relatively homogeneous in the three directions (X, Y, Z) and although the planes of anisotropy are visible to the naked eye due to the preferential direction of the lithic fragments, it does not seem that these generate planes of weakness which could affect this property.

Table 4 Results from ultrasound propagation velocity test

Ignimbrite		PWV (m/s)			
		Max	Min	Mean	SD
RS	*X*	5032.78	4956.93	4999.19	30.37
	Y	5093.43	4898.74	4996.22	81.44
	Z	4981.06	4815.20	4964.21	83.26
LT	*X*	4144.80	3707.30	3984.21	112.43
	Y	4278.40	3811.50	4072.83	138.63
	Z	4079.10	3826.00	3938.43	84.14

Colorimetry

Analysing the colour parameters obtained, it can be seen that the luminosity is practically the same in both samples, L* = 52.45 in the "*Rosa Silva*" ignimbrite and L* = 52.52 in the "*Lomo Tomás de León*" ignimbrite. The "*Rosa Silva*" ignimbrite, with a* = -1.18, tends to green, while the "*Lomo Tomás de León*" ignimbrite is closer to red, a* = 0.21. Regarding the parameter b*, the ignimbrite "*Lomo Tomás de León*" presents a b* = 2.91, higher than the one obtained in the ignimbrite "*Rosa Silva*", b* = 1.90, which means that

Table 5 Colour parameters

Ignimbrite	L*			a*			b*			C^*_{ab}			h_{ab}		
	Max	Min	Mean	Max	Min	Mean	Max	Min	Mean	Max	Min	Mean	Max	Min	Mean
RS	54.03	51.18	52.45	− 1.09	− 1.33	− 1.18	2.21	1.43	1.90	2.49	1.88	2.25	130.6	116.7	122.3
LT	55.33	46.91	52.52	0.51	0.05	0.21	3.49	2.48	2.91	3.53	2.48	2.92	89.04	81.62	86.06

RS Rosa Silva, *LT* Lomo Tomás de León, *L** lightness, *a** red-green value, *b** blue- yellow value, C^*_{ab} chroma value, h_{ab} hue value

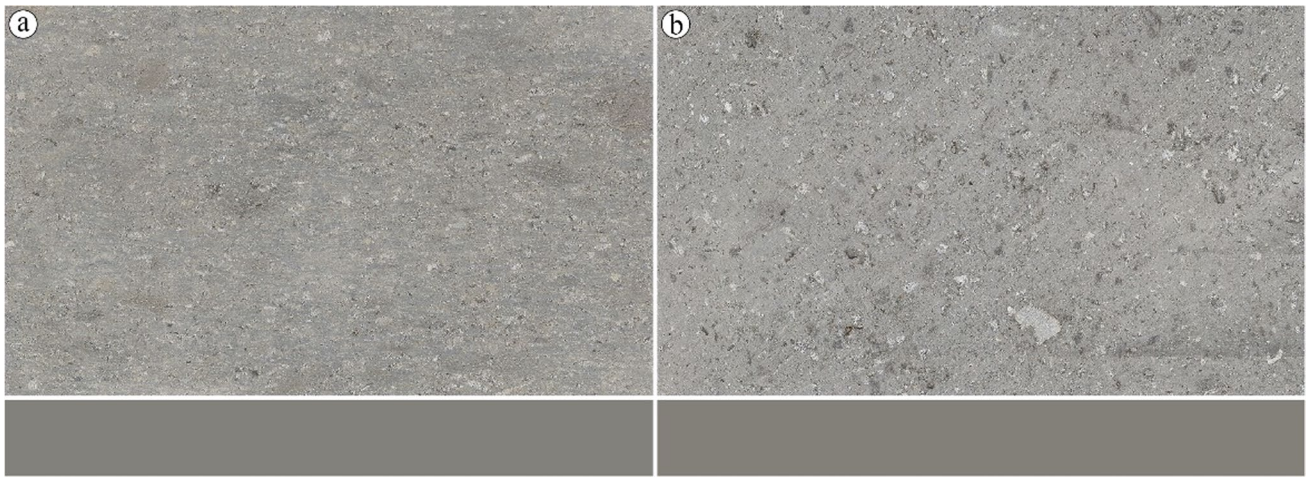

Fig. 14 Texture and mean measured colour (**a**) RS and (**b**) LT

Table 6 Results from uniaxial compressive strength (UCS) test

Ignimbrite		UCS (MPa)			
		Max	Min	Mean	SD
RS	*X*	92.66	50.33	67.34	12.73
	Z	84.53	50.84	69.82	10.02
LT	*X*	64.06	30.06	51.19	12.25
	Z	75.23	46.00	60.87	9.53

the ignimbrite "Lomo Tomás de León" tends more to yellow (Table 5).

The chromatic coordinates a* and b* of both samples are close to the centre of their respective axes (a* = 0 and b* = 0), as is the luminosity (L* = 50), this being the area of the CIELab colour space corresponding to the grey colours. The numerically calculated colour variation is ΔE* = 1.7 (Eq. 4). According to the value of ΔE* obtained, the colour difference between these two samples could only be perceived by an experienced observer and certainly the colours are very similar with a very subtle difference in hue that is difficult to appreciate with the naked eye (Fig. 14). However, the textural characteristics of each ignimbrite accentuate this difference and make them easily distinguishable.

Mechanical properties

Uniaxial compressive strength (UCS)

The mean values obtained for the compressive strength of the "*Rosa Silva*" ignimbrite is 67.34 MPa and 69.82 MPa depending on whether the load is applied parallel or perpendicular to the anisotropy planes, respectively. For the ignimbrite "*Lomo Tomás de León*" the results obtained for compressive strength is 51.19 MPa when the load is applied in the X-axis direction and 60.87 MPa when applied in the Z-axis direction (mean values, Table 6). The difference in compressive strength between the two test directions is most noticeable in the "*Lomo Tomás de León*" ignimbrite. In this sample, there is a slight tendency for higher strength when the load is applied perpendicular to the anisotropy planes. On the other hand, in the "*Rosa Silva*" ignimbrite, practically the same strength values were obtained for both test directions, even more so if the deviation of the results is taken into account. The difference in compressive strength between these two ignimbrites is not very significant, although the "Rosa Silva" ignimbrite seems to show a slightly higher compressive strength than the "*Lomo Tomás de León*" ignimbrite. However, according to the classification proposed by Anon (1979), both ignimbrites have a strong compressive strength. For these kinds of ignimbrites, which are welded tuffs, the compressive strength is highly dependent on the degree of welding, and therefore the range between minimum and maximum compressive strength data is very wide. Ignimbrites with compressive strengths between 5 and 7 MPa can be found in the literature (Teymen and Mengüç 2020; Çelik and Çobanoğlu 2019; Koralay and Çelik 2019; Kekec and Gokay 2009; Dinçer & Bostancı 2019), between 20 and 30 MPa (Koralay et al. 2011; Akbulut 2022; Türkdönmez and Bozcu 2012; Özbek 2014), close to 50 MPa (Özşen et al. 2017, Martínez-Martínez et al. 2018, Çelik and Aygün 2019) or at 100 MPa (Jamshidi et al. 2013a, b; Rodríguez-Losada et al. 2007). Some even with strengths above 140 MPa are reported (Engidasew 2014; Engidasew and Abay 2016; Ghobadi et al. 2016). According to the published data, the two ignimbrites of this study behave in accordance with their lithology, with a compressive strength between 50 and 70 MPa.

Table 7 Results from flexural strength (BS), point load test (PLT), splitting tensile strength (STS) and rupture energy (RE) test

Ignimbrite	FS (MPa)				PLT (MPa)				STS (MPa)				RE (J)			
	Max	Min	Mean	SD	Max	Min	Mean	SD	Max	Min	Mean	SD	Max	Min	Mean	SD
RS	18.51	15.96	17.15	1.00	9.98	5.79	7.82	1.56	13.95	11.90	13.25	1.18	5.95	4.96	5.55	0.41
LT	8.77	7.14	8.01	0.52	4.39	3.19	3.70	0.38	5.81	5.05	5.38	0.39	4.46	3.47	3.87	0.41

RS Rosa Silva, *LT* Lomo Tomás de León

Flexural strength under concentrated load (FS)

A mean value of 17.2 MPa was obtained for the flexural strength of "*Rosa Silva*", more than double that for the "*Lomo Tomás de León*" ignimbrite (8.0 MPa) (Table 7). This more than remarkable difference, confirms that the bending strength of the "*Rosa Silva*" ignimbrite is significantly higher than that of the "*Lomo Tomás de León*" ignimbrite. The flexural strength of this type of stone generally ranges between 1 and 7 MPa (Yüksek 2019, Yavuz et al. 2015, Bustamante et al. 2021, Akbulut 2022, Teymen 2018), ignimbrites with higher bending strengths are rare. For example, Careddu and Grillo (2019) report, in their study of a group of ignimbrites from different provinces of Sardinia (Italy), flexural strengths of 12.3 and 18.9 MPa and Çelik et al. (2014) obtained for a tuff from Turkey (Ayazini tuff) an average flexural strength of 15.8 MPa, however, these are punctual cases. The "*Lomo Tomás de León*" ignimbrite shows a bending strength slightly higher than the average strength found in the literature, while the bending strength of the "*Rosa Silva*" ignimbrite is among the highest strength values.

Point load strength (PLT)

The difference in point load resistance between the "*Rosa Silva*" ignimbrite and the "*Lomo Tomás de León*" ignimbrite is remarkable. The "*Rosa Silva*" ignimbrite shows an average point load resistance of 7.82 MPa, which is more than double the point load resistance obtained for the "*Lomo Tomás de León*" ignimbrite (3.70 MPa) (Table 7). According to the classification proposed by Selby (1980) ignimbrites are an example of lithology with moderate point load resistance, with stress values between 2.0 and 4.0 MPa.

The "*Lomo Tomás de León*" ignimbrite perfectly matches this description; however, the ignimbrite "*Rosa Silva*" presents a point load resistance, with maximum values (> 8 MPa), associated with other more resistant types of stone such as marble or gabbro. In fact, the "*Rosa Silva*" is one of a very small group of ignimbrites capable of overcoming a point load resistance of 4 MPa (Rodríguez-Losada et al. 2007; Engidasew 2014; Ghobadi et al. 2016), when the point load resistance of this type of stone is typically between 1.0—4.0 MPa (Kılıç and Teymen 2008, Bozdağ and İnce 2018, Özşen et al. 2017, Yavuz et al. 2015b, Topal and Sözmen 2001, Ince and Fener 2016).

Splitting tensile strength (STS)

The "*Rosa Silva*" ignimbrite has an average tensile strength of 13.25 MPa, which is significantly higher than that of the "*Lomo Tomás de León*" ignimbrite (5.38 MPa) (Table 7). Based on the results obtained by other authors, it can be seen that the tensile strength for this type of stone is generally between 1.0 and 4.5 MPa (Kılıç and Teymen 2008, Pötzl et al. 2018a, b, Ince and Fener 2016, Stück et al. 2008), this is also a similar range to that obtained by Pötzl et al. (2022) in their literature review. The "Lomo Tomás de León" ignimbrite has a tensile strength slightly above this range, however, it is a strength value within what would be expected, taking into account that ignimbrites with similar strengths can be found in the literature (Germinario and Török 2019; Kahraman et al. 2016). The "*Rosa Silva*" ignimbrite, on the other hand, is an atypical case, because, although it is possible to find ignimbrites with tensile strengths above 8 MPa (Jamshidi et al. 2013a, b; López-Doncel et al. 2016; López-Doncel et al. 2013) these are extreme cases that do not represent a normal distribution of the tensile strength of this lithotype.

Rupture energy (RE)

The rupture energy of the "*Rosa Silva*" ignimbrite (5.6 J) is higher than that of the "*Lomo Tomás de León*" ignimbrite (3.9 J) (Table 7). In terms of steel ball drop height, the "Rosa Silva" ignimbrite broke when the ball was dropped from an average height of 60 cm, while the drop height for the "*Lomo Tomás de León*" ignimbrite did not exceed 40 cm. According to the classification proposed by Sarıışık (2016), the ignimbrite "*Lomo Tomás de León*" has a low rupture potential (rupture energy 3.5–4.0 J), while for "*Rosa Silva*" ignimbrite is extremely low (rupture energy > 4.0 J). This property is of particular interest when the stone is to be used as paving, which is one of its most frequent applications (Kundak et al. 2020). However, it is not a test that is routinely included

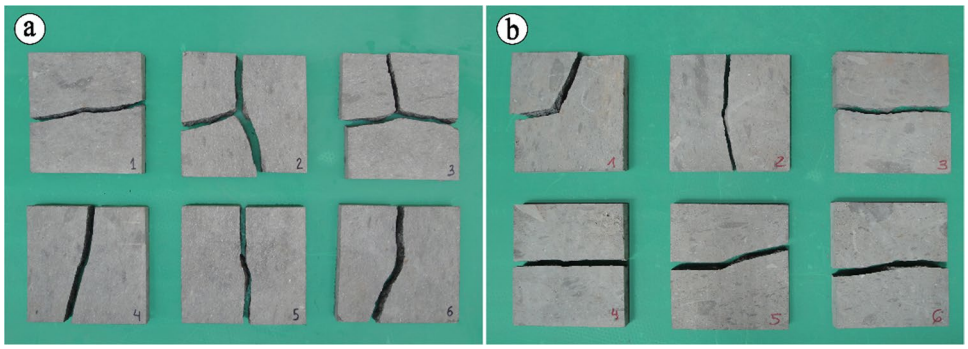

Fig. 15 Fracture of specimens after testing (**a**) RS and (**b**) LT

Table 8 Results from abrasion resistance (WWA), resistance to salt crystallisation (SC) and resistance to ageing by salt mist (SM) test

Ignimbrite	WWA (mm)				SC (%)				SM (%)			
	Max	Min	Mean	SD	Max	Min	Mean	SD	Max	Min	Mean	SD
RS	15.64	14.71	15.33	0.34	0.55	0.13	0.26	0.15	0.17	− 0.03	0.10	0.07
LT	20.84	19.16	19.87	0.57	− 2.21	− 6.21	− 5.03	1.52	0.04	0.04	0.04	0.00

RS Rosa Silva, *LT* Lomo Tomás de León

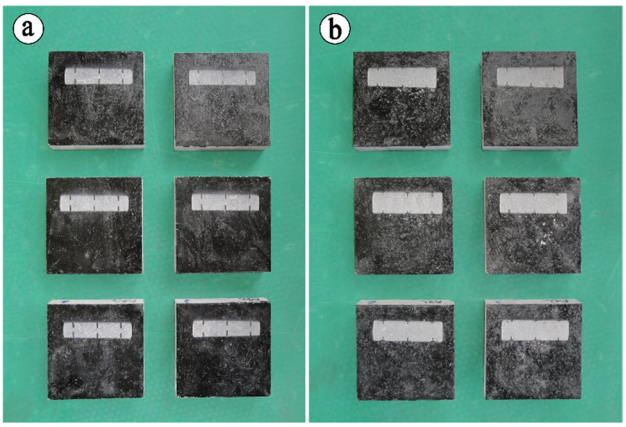

Fig. 16 Footprint of specimens after testing (**a**) RS and (**b**) LT

in research, so the available literature is small compared to other properties. Granite, with an average rupture energy of 6.0 J (Costa et al. 2021; Simão et al. 2010; Isabel and Borges 2019), limestone with 4.2 (Laskaridis et al. 2021; Costa et al. 2021, Karakaş et al. 2021) and marble with 4.8 J (Laskaridis et al. 2021; Allocca et al. 2010; Costa et al. 2021) are the most studied stone types with regard to this property. Figure 15 shows the specimen rupture after the test, which preferable occurs parallel to weakness planes.

Durability assessment

Abrasion resistance (WWA)

The mean width of the track produced by the abrasive disc on the surface of the "*Rosa Silva*" ignimbrite is 15.3 mm, lower than the wear on the "*Lomo Tomás de León*" ignimbrite, with a mean track width of 19.9 mm (Table 8; Fig. 16). According to the data found in the literature, the abrasion resistance of this type of stone is usually in the range 20–50 mm (Yavuz et al. 2015b, Careddu and Grillo 2019, Çelik and Çobanoğlu 2019; Özvan and Direk 2021; Engidasew 2014). The "*Lomo Tomás de León*" ignimbrite, although at the lower limit, is within this range, while the ignimbrite "*Rosa Silva*" presents a higher resistance to abrasion, similar to that of other types of stone a priori more resistant than ignimbrites, such as granites whose resistance to abrasion ranges between 13 and 18 mm. (Karaca et al. 2010, 2012, Çelik and Çobanoğlu 2019, Sousa 2014). Abrasion resistance is a property to consider when assessing the suitability of a natural stone used as a pavement (Marradi et al. 2008), especially in areas subjected to heavy traffic, whether vehicular or pedestrian (Çelik and Çobanoğlu 2022). It should also be taken into account when assessing the wear of the machinery used in the quarries for the extraction of the blocks and the cutting tools used in their further processing (Kolgitti and Çelik 2022).

Resistance to salt crystallisation (SC)

The resistance to crystallisation of the salts is evaluated through the variation between the initial mass of the specimen and the final mass at the end of the test (after 15 cycles). In most cases, this variation represents a weight loss (DWL), produced by grain saltation and decohesion (Cardell et al. 2003), as in the case of the ignimbrite "*Lomo Tomás de León*", with a weight loss of 5% (Table 8). However, depending on the mineralogical composition and pore morphology, the number of cycles established by the standard may not be

sufficient to detect, in terms of mass loss, the degradation of the sample. In fact, many authors have doubled the number of cycles in their research (Buj and Gisbert 2010; Alvarez de Buergo et al. 2015; Germinario and Török 2019; Benavente et al. 2018; Tel & Sarıışık 2020, Martínez-Martínez et al. 2018) or prolonged the test by the number of cycles needed to induce a 30% weight loss in the sample (López-Doncel et al. 2016; Pötzl et al. 2018a, b; Siegesmund et al. 2018). If, at the end of the test, the degree of deterioration achieved is not sufficient to cause a loss of material, what is recorded is an increase in mass, generally negligible, due to the deposition of salts in the cavities and that have not been dissolved in the subsequent washes (Angeli et al. 2006). This is the case for the ignimbrite "*Rosa Silva*" whose mass increased by 0.2% (Table 9). The behaviour of this type of stone with respect to salt crystallisation is so disparate that ignimbrites with a mass loss of less than 5% can be found alongside others with a loss of more than 80% (Çelik and Aygün 2018, Özşen et al. 2017b, Martínez-Martínez et al. 2018). May be even degrade completely in the third cycle (Yavuz 2012) or between the eighth and ninth cycles (Çelik and Sert 2020). Compared to the literature data, the ignimbrites in this study are among the most resistant to salt crystallisation. It should be noted that crystallisation of salts in one of the main mechanisms of deterioration of both cultural heritage and modern buildings (Çelik and Sert 2021; Jamshidi et al. 2013a, b) being sodium sulphate one of the most aggressive agents because the strong crystallisation pressure (Cultrone and Sebastián 2008).

Resistance to ageing by salt mist (SM)

The weight variation obtained in both the "*Rosa Silva*" ignimbrite (0.04%) and the "*Lomo Tomás de León*" ignimbrite (0.10%) is not very significant (Table 8). According to Flatt et al. (2017), the damage caused by salt crystallisation is divided into two phases; the induction phase, where salts accumulate in the porous system of the material and the propagation phase, where dissolution/crystallisation cycles begin. The results obtained, mass gain in both samples, seem to indicate that the number of cycles established in the standard (60 cycles) is not sufficient, in this case, to pass from the propagation phase, so the volume of salt occupying the pores is not high enough to initiate damage and cause the loss of material. According to the published results, the weight loss in this test is usually negligible or even non-existent for any type of stone. The following the results are found in literature, andesites with mass losses of less than 0.50% (Çelik et al. 2019a, 2021), tuffs with a mass loss of 0.30% (Çelik et al. 2019b), limestones and sandstones with a maximum mass loss of 1% (Carvalho et al. 2018; Simão et al. 2015; Kłopotowska and Łukaszewski 2014, Cantisani et al. 2013). Some authors increase the number of cycles considerably in order to cause sufficient deterioration to be able to analyse their effects. Simão et al. (2011) subjected a group of limestones and granites to 90 cycles, and even then the mass loss did not exceed 1%. Buergo et al. (2015) in their study of limestone from Colmenar (Madrid), goes up to 120 cycles and obtains an average mass loss of 0.5%. Borges et al. (2011) continue the test up to 150 cycles and the mass loss obtained, in different granites, is less than 0.25%. Visual analysis of the samples also shows no evidence of damage. The edges of the cubes are perfectly defined and have not even lost the marks made before starting of the test. Surfaces show no discolouration or efflorescence (Fig. 17). The lack of mass loss and the absence of surface damage give these ignimbrites a good resistance to salt

Table 9 Results from Resistance to ageing by SO_2 action (SO) test

Ignimbrite		SO (%)			
		Max	Min	Mean	SD
RS	*A*	0.13	− 0.02	0.06	0.07
	B	0.08	0.01	0.05	0.04
LT	*A*	0.11	0.05	0.07	0.03
	B	0.08	0.04	0.05	0.03

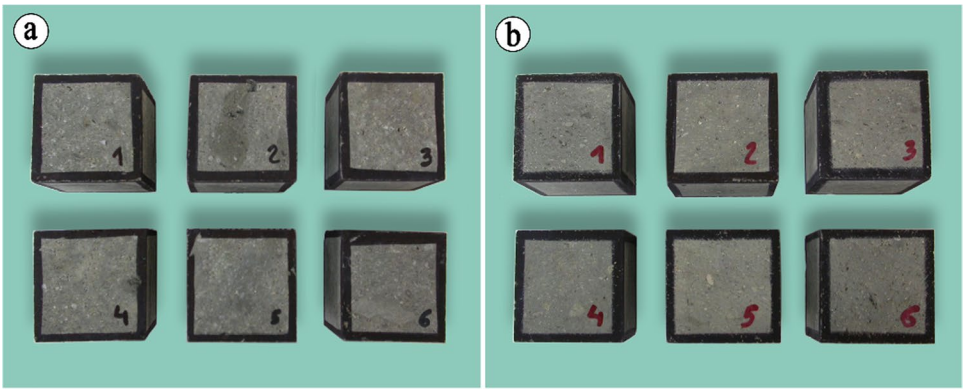

Fig. 17 Condition of specimens after 60 salt mist cycles (**a**) RS and (**b**) LT

spray ageing. This is important, as the main destination of these building stones is construction sites located within the island environment and this test is intended to simulate the atmosphere to which the stone is exposed in coastal environments, areas up to 20 km away from the coastline due to the dispersion of marine aerosols (Fonseca 2012).

Resistance to ageing by SO_2 action in the presence of humidity

The ignimbrites "*Rosa Silva*" and *"Lomo Tomás de León*" show similar resistance to SO_2 ageing. Both samples gain weight in similar proportions, although the average mass variation is insignificant, between 0.05 and 0.07% depending on the concentration of the solution. The difference between solution A and solution B is also insignificant, with a difference of 0.01% for the "*Rosa Silva*" ignimbrite and 0.02% for "*Lomo Tomás de León*" (Table 9). According to Schiavon (2007), weathering caused by exposure to an acidic atmosphere (SO_2) is due to the kaolinisation of minerals rich in sodium (Na), calcium (Ca) and potassium (K), such as feldspars, and the sulphation of minerals with calcium (Ca) in their composition. Oxidation of ferromagnesian minerals by SO_2 deposition is another mechanism that may be involved in stone degradation.

In summary, the degree of weathering will largely depend on petrophysical properties, porosity and mineralogical composition, primarily (Fort 2007). Due to the great heterogeneity of these properties, it is possible to find limestones that gain 0.50% (Solution A) / 0.10% (Solution B) weight (Ortega-Díaz et al. 2014) and others that lose 1.72% (Solution A) / 0.31% (Solution B) (Karakaş et al. 2021). Sandstones that lose 1.15% (Solution A) / 0.95% (Solution B) (Selim et al. 2019) and others that suffer practically no variation − 0.04% (Solution A) / − 0.11% (Solution B) are mentioned by Molina et al. (2020). Although in the reviewed literature there are numerous studies where this ageing test is used to determine the deterioration of the stone, it should be noted that in many of these studies the procedure described in the UNE-EN 13919 standard (AENOR 2003) is modified, a fact that is also highlighted by Çetintaş and Akboğa (2020), and which makes it difficult or impossible to make a comparison in the same terms. Gibeaux et al. (2018) use different SO_2 / NO_x ratios as acid, Romero et al. (2022) prepare a single solution with a concentration of 60% and (Hazrathosseini and Mahdevari 2018) measure ageing resistance from softening depth, among others. The resistance to ageing by the action of SO_2 of the "*Rosa Silva*" and the "*Lomo Tomás de León*" ignimbrites is similar to that of the marble studied by Ortega-Díaz et al. (2014), 0.08% (Solution A) / 0.04% (Solution B) or to the limestone studied by Çetintaş et al. (2022) 0.07% (Solution A) / 0. 04% (Solution B), while it presents a completely different behaviour to the tuff studied by Çelik et al. (2019a, b) which also suffers, like tuff, a mass loss, 0.74% (Solution A) / 0.14% (Solution B). Visual analysis assess the presence of fouling, discolouration, efflorescence or black crusts on the surface of the stone, the latter being one of the most typical formations of exposure to this type of acidic environment, especially in carbonate rocks (Lefèvre and Ausset 2002). According to the magnitude of the mass variation obtained and the lack of indicators of surface deterioration of the specimens, a good resistance to SO_2 ageing is assumed. The aim of this property is to simulate anthropogenic contamination in order to evaluate the behaviour of the stone in corrosive environments. Although the location of the existing works and their potential use is far from large cities with intense traffic or high industrialisation, it should be noted that current logistics make it possible exporting this stone to be used anywhere in the world.

General considerations

According to the above properties, summarised in Table 10, both varieties show values within the range of these stones. However, the "Rosa Silva" variety has lower porosity and higher resistance to the durability tests. Furthermore, both are texturally homogeneous as demonstrated by the values of the properties obtained in the orthogonal directions.

The weathering conditions of the monumental heritage found on the Canary Islands and elsewhere proves the quality of this ignimbrite as a building stone. Both varieties can be used as a building stone, with the mandatory adequation to the specific utilization and place. As stated above, the high porosity of the LT variety enables their use when water and/or salt can affect the stone evolution.

The results obtained are also useful for the rehabilitation works and maintenance of local architectural characteristics. The available places for extracting building stones are scarce because the low number of available outcrops and also as a consequence of the legal constrains that avoids the extraction of most of the island areas.

The quarrying activity is important is low-income regions, as the Canary Islands. Therefore, the study of the properties of these building stones are key factor for the sustainable development and local / regional economy.

In the Canary archipelago only nine building stones are extracted, distributed in three islands. The study and characterisation are basic steps for the maintenance of this activity. This research intends to be a step towards the recognition of the social and economic importance connected to quarry activity and a contribution to the designation of "*Piedra Chasnera*" as Global Heritage Stone Resource (GHSR).

Table 10 Summary of the physical and mechanical properties

Test	RS	LT
Physical properties		
Apparent density [g/cm^3]	$2.38^{\pm 0.01}$	$2.05^{\pm 0.02}$
Open porosity [%]	$3.20^{\pm 0.53}$	$22.10^{\pm 0.71}$
Water absorption at atmospheric pressure [%]	$2.67^{\pm 0.17}$	$7.32^{\pm 0.72}$
Water absorption coefficient by capillarity [g/m^2·s$^{0.5}$]—X	$7.76^{\pm 1.57}$	$19.80^{\pm 2.41}$
Water absorption coefficient by capillarity [g/m^2·s$^{0.5}$]—Z	$6.37^{\pm 1.68}$	$16.94^{\pm 2.75}$
Ultrasound propagation velocity [m/s]—X	$4999.2^{\pm 30.4}$	$3984.2^{\pm 112.4}$
Ultrasound propagation velocity [m/s]—Y	$4996.2^{\pm 81.4}$	$4072.8^{\pm 138.6}$
Ultrasound propagation velocity [m/s]—Z	$4964.2^{\pm 83.3}$	$3983.4^{\pm 84.1}$
Total anisotropy index [%]	0.67	2.24
Relative anisotropy index [%]	0.06	2.20
Mechanical properties		
Uniaxial compressive strength [MPa]—X	$67.34^{\pm 12.73}$	$51.19^{\pm 12.25}$
Uniaxial compressive strength [MPa]—Z	$69.82^{\pm 10.02}$	$60.87^{\pm 9.53}$
Flexural strength under concentrated load [MPa]	$17.15^{\pm 1.00}$	$8.01^{\pm 0.52}$
Point load strength [MPa]	$7.82^{\pm 1.56}$	$3.70^{\pm 0.38}$
Splitting tensile strength [MPa]	$13.25^{\pm 1.18}$	$5.38^{\pm 0.39}$
Rupture energy [J]	$5.55^{\pm 0.41}$	$3.87^{\pm 0.41}$
Durability		
Abrasion resistance [mm]	$15.33^{\pm 0.34}$	$19.87^{\pm 0.57}$
Resistance to salt crystallisation [%]	$0.26^{\pm 0.15}$	$-5.03^{\pm 1.52}$
Resistance to ageing by salt mist [%]	$0.10^{\pm 0.07}$	$0.04^{\pm 0.00}$
Resistance to ageing by SO2 action [%]—Solution A	$0.06^{\pm 0.07}$	$0.07^{\pm 0.03}$
Resistance to ageing by SO2 action [%]—Solution B	$0.05^{\pm 0.04}$	$0.05^{\pm 0.03}$

Acknowledgements We are grateful to the "Servicio de Laboratorios y Calidad de la Construcción del Gobierno de Canarias" for their collaboration in the execution of the tests, to the "Cantería de Arucas S.L" quarry for providing the necessary samples in order to carry out this study and to Prof. Dr. Rui Teixeira for his help with the petrographic description. The X-Ray Fluorescence tests were financed through the Nuclear Safety Council PR32960 "Radon emission in the volcanic materials of the Canary Islands. Implications for residential infrastructures and public works" project. This study was supported by the "Fundação para a Ciência e a Tecnologia" in the frame of the UIDB/00073/2020 and UIDP/00073/2020 projects of the I&D unit Geosciences Center (CGEO) and by the Ministry of Universities of Spain, through the pre-doctoral contract of the first author (FPU16/05739).

Author contributions JV: conceptualization, analysis, investigation, writing, editing. JC: conceptualization, supervision and reviewing. LS: conceptualization, writing and reviewing.The first draft of the manuscript was written by JV and all authors commented on previous versions of the manuscript. All authors read and approved the final manuscript.

Funding Open Access funding provided thanks to the CRUE-CSIC agreement with Springer Nature.

Data Availability Data available on request from the authors.

Declarations

Competing interests The authors declare no competing interests.

References

Angeli M, Bigas JP, Benavente D et al (2007) Salt crystallization in pores: quantification and estimation of damage. Environ Geol 52:205–213. https://doi.org/10.1007/s00254-006-0474-z

AENOR (2007d) EN 1936. Natural stone test methods. Determination of real density and apparent density, and of total and open porosity.

AENOR (2007c) EN 1926. Determination of uniaxial compressive strength, Natural stone test methods

AENOR (2008a) EN 13755. Determination of water absorption at atmospheric pressure, Natural stone test methods

AENOR (1990) UNE 22950–1. Mechanical properties of rocks. Strength determination tests. Part 1: Uniaxial compressive strength.

AENOR (2003) EN 13919. Natural stone test methods - Determination of resistance to ageing by SO2 action in the presence of humidity.
AENOR (2004a) EN 14147. Natural stone test methods - Determination of resistance to ageing by salt mist.
AENOR (2004b) EN 14158. Natural stone test methods. Determination of rupture energy.
AENOR (2005a) EN 14157. Natural stone test methods. Determination of the abrasion resistance.
AENOR (2005b) EN 14579. Natural stone test methods. Determination of sound speed propagation.
AENOR (2007a) EN 12372. Natural stone test methods. Determination of flexural strength under concentrated load.
AENOR (2007b) EN 12407. Natural stone test methods. Petrographic examination.
AENOR (2008b) EN 15309. Characterization of waste and soil - Determination of elemental composition by X-ray fluorescence.
AENOR (2011) EN 15886. Conservation of cultural property - Test methods - Colour measurement of surfaces.
AENOR (2020) EN 12370. Natural stone test methods. Determination of resistance to salt crystallisation.
Ahmed I, Basharat M, Sousa L et al (2021) Evaluation of building and dimension stone using physico-mechanical and petrographic properties: a case study from the Kohistan and Ladakh batholith, Northern Pakistan. Environ Earth Sci 80:1–17. https://doi.org/10.1007/S12665-021-10007-Y/TABLES/5
Ajanaf T, Gómez Grás D, Navarro A et al (2020) The building stone of the Roman city of Lixus (NW Morocco): provenance, petrography and petrophysical characterization. Geol Acta 18(13):1–16. https://doi.org/10.1344/GEOLOGICAACTA2020.18.13
Akbulut ZF (2022) Investigation of the change in physical, mechanical, and microstructural properties of Ahlat ignimbrites under the effect of environment and freeze-thawing. Arab J Geosci 156:1–11. https://doi.org/10.1007/S12517-022-09779-9
Akın M, Özvan A, Dinçer İ et al (2017) Evaluation of the physico-mechanical parameters affecting the deterioration rate of Ahlat ignimbrites (Bitlis, Turkey). Environ Earth Sci 76. https://doi.org/10.1007/s12665-017-7175-7
Allocca F, Calcaterra D, Calicchio G et al (2010) Ornamental stones in the cultural heritage of Campania region (southern Italy): The Vitulano marbles. Geol Soc Spec Publ 333:219–231. https://doi.org/10.1144/SP333.21
Buergo MA, Fort R, Varas-Muriel MJ et al (2015) Colmenar Limestone, Madrid, Spain: Considerations for its nomination as a global heritage stone resource due to its long term durability. Geol Soc Spec Publ 407:121–135. https://doi.org/10.1144/SP407.8
Alves R, Faria P, Simão J (2017) Experimental characterization of a Madeira Island basalt traditionally applied in a regional decorative mortar. J Build Eng 13:326–335. https://doi.org/10.1016/j.jobe.2017.09.004
Anguita F, Hernán F (2000) The Canary Islands origin: a unifying model. J Volcanol Geotherm Res 103:1–26. https://doi.org/10.1016/S0377-0273(00)00195-5
ANON (1979) Classification of rocks and softs for engineering geological mapping. Part 1: Rock and soil materials. (IAEG Commission of engineering geological mapping). Bull Int Assoc Engng Geol 19:364–371
ANON (1981) Basic geotechnical description of rock masses. (ISRM Commission on classification of rocks and rock masses). Int J Rock Mech Min Sci 18:85–110
Anon (1979) Classification of rocks and soils for engineering geological mapping. Bull Eng Geol Environ 364–371. https://doi.org/10.1007/BF02600503
ASTM (2016a) D3967-16 Standard Test Method for Splitting Tensile Strength of Intact Rock Core Specimens.
ASTM (2016b) D5731–16. Determination of the Point Load Strength Index of Rock andApplication to Rock Strength Classifications.
Balcells RJ, Barrera JL, Gómez JA et al (1992) Memoria escala 1:100000 de la isla de Gran Canaria. Primera
Barbero-Barrera MM, Flores-Medina N, Moreno-Fernández E (2019) Thermal, physical and mechanical characterization of volcanic tuff masonries for the restoration of historic buildings. Mater Construcción 69:e179. https://doi.org/10.3989/MC.2019.12917
Bas MJL, Maitre RWL, Streckeisen A et al (1986) A chemical classification of volcanic rocks based on the total alkali-silica diagram. J Petrol 27:745–750. https://doi.org/10.1093/petrology/27.3.745
Benavente D, Martinez-Martinez J, Cueto N et al (2018) Impact of salt and frost weathering on the physical and durability properties of travertines and carbonate tufas used as building material. Environ Earth Sci 77:1–13. https://doi.org/10.1007/S12665-018-7339-0/FIGURES/5
Bogdanowitsch M, Sousa L, Siegesmund S (2022) Building stone quarries: resource evaluation by block modelling and unmanned aerial photogrammetric surveys. Environ Earth Sci 81:1–55. https://doi.org/10.1007/S12665-021-10031-Y/TABLES/6
Borges M, Simão J, Silva Z (2011) Artificial Weathering of Portuguese Granites Exposed to Salt Atmosphere: Variations of Physico-Mechanical Properties. In: Proceedings of the Conference on Salt Weathering on Buildings and Stone Sculptures.
Bozdağ A, Ince İ (2018) Predicting Strength Parameters of Igneous Rocks from Slake Durability Index. Afyon Kocatepe Üniversitesi Fen Ve Mühendislik Bilim Derg 18:1102–1109. https://doi.org/10.5578/fmbd.67821
Buj O, Gisbert J (2010) Influence of pore morphology on the durability of sedimentary building stones from Aragon (Spain) subjected to standard salt decay tests. Environ Earth Sci 61:1327–1336. https://doi.org/10.1007/S12665-010-0451-4/TABLES/7
Bustamante R, Vazquez P, Prendes N (2021) Properties of the Ignimbrites in the Architecture of the Historical Center of Arequipa, Peru Appl Sci, 11 10571 11:10571. https://doi.org/10.3390/APP112210571
Byerly DW, Knowles SW (2017) Tennessee "Marble": a potential "Global Heritage Stone Resource". Episodes J Int Geosci 40:325–331. https://doi.org/10.18814/EPIIUGS/2017/V40I4/017033
Cabrera M (1985) Estratigrafía y sedimentología del sector meridional de la terraza sedimentaria de Las Palmas (Gran Canaria, Islas Canarias). University of Salamanca https://books.google.es/books?id=agyyswEACAAJ
Cardell C, Rivas T, Mosquera MJ et al (2003) Patterns of damage in igneous and sedimentary rocks under conditions simulating sea-salt weathering. Earth Surf Process Landforms 28:1–14. https://doi.org/10.1002/ESP.408
Cárdenes V, Cabrera-Guillén D, López-Piñeiro S et al (2022) The Historical Significance of the Welded Tuffs from Arucas, Canary Islands. Geoheritage 14:1–10. https://doi.org/10.1007/S12371-022-00680-1/FIGURES/6
Careddu N, Grillo SM (2019) "Trachytes" from Sardinia: Geoheritage and Current Use. Sustain 2019, Vol 11, Page 3706 11:3706. https://doi.org/10.3390/SU11133706
Careddu N, Grillo SM (2015) Rosa Beta granite (Sardinian Pink Granite): a heritage stone of international significance from Italy. Geol Soc Spec Publ 407:155–172. https://doi.org/10.1144/SP407.1
Carracedo JC, Day SJ, Guillou H et al (1998) Hotspot volcanism close to a passive continental margin: the Canary Islands. Geol Mag 135:591–604. https://doi.org/10.1017/S0016756898001447

Carracedo JC, Pérez FJ, Ancochea E et al (2002) Cenozoic volcanism II: the Canary Islands. In: The Geology of Spain. London, GS of, editor. pp 439–472

Cantisani E, Garzonio CA, Ricci M, Vettori S (2013) Relationships between the petrographical, physical and mechanical properties of some Italian sandstones. Int J Rock Mech Min Sci 60:321–332. https://doi.org/10.1016/j.ijrmms.2012.12.042

Carvalho J, Lisboa J, Moura A et al (2013) Evaluation of the portuguese ornamental stone resources. Key Eng Mater 548:3–9. https://doi.org/10.4028/WWW.SCIENTIFIC.NET/KEM.548.3

Carvalho C, Silva Z, Simão J (2018) Evaluation of Portuguese limestones' susceptibility to salt mist through laboratory testing. Environ Earth Sci 77:1–15. https://doi.org/10.1007/S12665-018-7670-5/TABLES/18

Cassar J, Torpiano A, Zammit T et al (2017) Proposal for the nomination of Lower Globigerina Limestone of the Maltese Islands as a "Global Heritage Stone Resource". Episodes J Int Geosci 40:221–231. https://doi.org/10.18814/EPIIUGS/2017/V40I3/017025

Çelik MY, Aygün A (2018) The effect of salt crystallization on degradation of volcanic building stones by sodium sulfates and sodium chlorides. Bull Eng Geol Environ 78:3509–3529. https://doi.org/10.1007/S10064-018-1354-Y

Çelik MY, Aygün A (2019) The effect of salt crystallization on degradation of volcanic building stones by sodium sulfates and sodium chlorides. Bull Eng Geol Environ 78:3509–3529. https://doi.org/10.1007/S10064-018-1354-Y/FIGURES/18

Çelik SB, Çobanoğlu İ (2019) Comparative investigation of Shore, Schmidt, and Leeb hardness tests in the characterization of rock materials. Environ Earth Sci 78:1–16. https://doi.org/10.1007/S12665-019-8567-7/FIGURES/13

Çelik MY, Ergül A (2015) The influence of the water saturation on the strength of volcanic tuffs used as building stones. Environ Earth Sci 74:3223–3239. https://doi.org/10.1007/S12665-015-4359-X/FIGURES/21

Çelik MY, Sert M (2020) The role of different salt solutions and their concentration ratios in salt crystallization test on the durability of the Döğer tuff (Afyonkarahisar, Turkey) used as building stones of cultural heritages. Bull Eng Geol Environ 79:5553–5568. https://doi.org/10.1007/S10064-020-01896-7/FIGURES/20

Çelik MY, Akbulut H, Ergül A (2014) Water absorption process effect on strength of Ayazini tuff, such as the uniaxial compressive strength (UCS), flexural strength and freeze and thaw effect. Environ Earth Sci 71:4247–4259. https://doi.org/10.1007/S12665-013-2819-8/FIGURES/15

Çelik MY, Ersoy M, Sert M et al (2021) Investigation of some atmospheric effects in the laboratory tests on deterioration of andesite (Iscehisar-Turkey) used as the building stone of cultural heritages. Arab J Geosci 14:1–20. https://doi.org/10.1007/S12517-020-06339-X/FIGURES/19

Çelik SB, Çobanoğlu İ (2022) Modelling and estimation of Wide Wheel abrasion values of building stones by multivariate regression and artificial neural network analyses. J Build Eng 45:103443. https://doi.org/10.1016/J.JOBE.2021.103443

Çelik MY, Sert M (2021) An assessment of capillary water absorption changes related to the different salt solutions and their concentrations ratios in the Döğer tuff (Afyonkarahisar-Turkey) used as building stone of cultural heritages. J Build Eng 35:102102. https://doi.org/10.1016/J.JOBE.2020.102102

Çelik MY, Arsoy Z, Sert M (2019a) Tuz buharının Döğer (İhsaniye-Afyonkarahisar) tüfüne etkisinin incelenmesi. In: Proceedings of the 26th International Mining Congress and Exhibition of Turkey. Maden Mühendisleri Odası pp. 1446–1456. http://acikerisim.aku.edu.tr/xmlui/handle/11630/7867. Accessed Mar 10, 2023

Çelik MY, Sert M, Arsoy Z (2019b) Investigation of the Effect of SO2 on the Deterioration of Döğer (İhsaniye-Afyonkarahisar) Tuff Used as Building Stone. In: 1st International Symposium on Innovations in Civil Engineering and Technology. pp. 26–48.

Celik SE, Gulen J, Viles HA (2020) Evaluating the effectiveness of DAP as a consolidant on Turkish building stones. Constr Build Mater 262:120765. https://doi.org/10.1016/J.CONBUILDMAT.2020.120765

Çetintaş S, Bağcı M, Yıldız A et al (2022) Degradation of limestone used as building materials under the influence of H2SO3 and HNO3 acids. Environ Earth Sci 81:1–21. https://doi.org/10.1007/S12665-022-10592-6/FIGURES/13

Çetintaş S, Akboğa Z (2020) Investigation of resistance to ageing by SO2 on some building stone. Constr Build Mater 262:120341. https://doi.org/10.1016/J.CONBUILDMAT.2020.120341

Costa FP et al. (2021) The potential for natural stones from northeastern Brazil to be used in civil construction. Miner 11:440. https://doi.org/10.3390/MIN11050440

Cueto N, Vieira-Sousa JF, Fernandes C et al. (2018) Water transport in lapilli tuff from Madeira Iland, Portugal: implications on degradation mechanisms and durability. https://digital.csic.es/handle/10261/189991. Accessed 15 Nov 2022

Cultrone G, Sebastián E (2008) Laboratory simulation showing the influence of salt efflorescence on the weathering of composite building materials. Environ Geol 56:729–740. https://doi.org/10.1007/S00254-008-1332-Y/FIGURES/9

Dinçer İ, Bostancı M (2019) Capillary water absorption characteristics of some Cappadocian ignimbrites and the role of capillarity on their deterioration. Environ Earth Sci 78:1–18. https://doi.org/10.1007/S12665-018-7993-2/FIGURES/10

Engidasew TA, Abay A (2016) Assessment and evaluation of volcanic rocks used as construction materials in the city of Addis Ababa. Momona Ethiop J Sci 8:193. https://doi.org/10.4314/mejs.v8i2.7

Engidasew TA (2014) Engineering geological characterization of volcanic rocks of ethiopian and sardinian highlands to be used as construction materials.***

Feng C, Janssen H (2018) Hygric properties of porous building materials (III): Impact factors and data processing methods of the capillary absorption test. Build Environ 134:21–34. https://doi.org/10.1016/J.BUILDENV.2018.02.038

Feraud G et al (1981) New K-Ar ages, chemical analyses and magnetic data of rocks from the islands of santa maria (azores), porto santo and madeira (madeira archipelago) and gran canaria (Canary Islands). Bull Volcanol 44:359–375. https://doi.org/10.1007/BF02600570/METRICS

Flatt R, Aly Mohamed N, Caruso F et al (2017) Predicting salt damage in practice: A theoretical insight into laboratory tests. RILEM Tech Lett 2:108–118. https://doi.org/10.21809/RILEMTECHLETT.2017.41

Fort R (2007) La contaminación atmosférica en el deterioro del patrimonio monumental: medidas de prevención. Ciencia, Tecnol y Soc para una Conserv Sosten del Patrim pétreo, pp 57–71. https://digital.csic.es/handle/10261/8322. Accessed 14 Mar 2023

Freire-Lista DM, Fort R, Varas-Muriel MJ (2015b) Freeze–thaw fracturing in building granites. Cold Reg Sci Technol 113:40–51. https://doi.org/10.1016/J.COLDREGIONS.2015.01.008

Freire-Lista DM, Fort R, Varas-Muriel MJ (2016) Thermal stress-induced microcracking in building granite. Eng Geol 206:83–93. https://doi.org/10.1016/J.ENGGEO.2016.03.005

Freire-Lista DM, Fort R, Varas-Muriel MJ (2015a) Alpedrete granite (Spain). A nomination for the "Global Heritage Stone Resource" designation. Episodes J Int Geosci 38:106–113. https://doi.org/10.18814/EPIIUGS/2015/V38I2/006

Freire-Lista DM, Sousa L, Carter R, Al-Na'īmī F (2021) Petrographic and petrophysical characterisation and structural function of

the heritage stones in Fuwairit Archaeological Site (NE Qatar): implications for heritage conservation. Episodes J Int Geosci 44:43–58. https://doi.org/10.18814/EPIIUGS/2020/0200S12

Freundt A, Schmincke HU (1995) Eruption and emplacement of a basaltic welded ignimbrite during caldera formation on Gran Canaria. Bull Volcanol 56:640–659. https://doi.org/10.1007/BF00301468

Fúster J, Hernñandez-Pacheco A, Muñoz M et al (1968) Geologia y volcanologia de las Islas Canarias: Gran Canaria. Inst Lucas Mallada CSIC 243. https://info.igme.es/biblio/bbiblio_Backup_2010_07_01/presentacion.asp?Id=71962. Accessed 22 Nov 2022

Gabaldón V, Cabrera MC, Cueto LA (1989) Formación detrítica de Las Palmas. Sus facies y evolución sedimentológica. In: Meeting on Canarian volcanism. Lanzarote.

Germinario L, Török Á (2019) Variability of technical properties and durability in volcanic tuffs from the same quarry region—examples from Northern Hungary. Eng Geol 262:105319. https://doi.org/10.1016/J.ENGGEO.2019.105319

Ghobadi MH, Taleb Beydokhti AR, Nikudel MR et al (2016) The effect of freeze–thaw process on the physical and mechanical properties of tuff. Environ Earth Sci 75:1–15. https://doi.org/10.1007/S12665-016-5664-8/FIGURES/10

Gibeaux S, Thomachot-Schneider C, Eyssautier-Chuine S, Marin B, Vazquez P (2018) Simulation of acid weathering on natural and artificial building stones according to the current atmospheric SO2/NOxrate. Environ Earth Sci 77:1–19. https://doi.org/10.1007/S12665-018-7467-6/TABLES/5

Guillén DC (2006) El oficio de la piedra en Arucas y su puesta en valor como recurso turístico. Universiidad de La Palmas de Gran Canaria

Guyader J, Denis A (1986) Propagation des ondes dans les roches anisotropes sous contrainte évaluation de la qualité des schistes ardoisiers. Bull Int Assoc Eng Geol 33:49–55. https://doi.org/10.1007/BF02594705

Hazrathosseini A, Mahdevari S (2018) Applicability quality assessment of dimension stones for service in the buildings (A new approach using a mathematical model and fuzzy logic). J Build Eng 20:585–594. https://doi.org/10.1016/J.JOBE.2018.09.002

Heiken G (2006) Tuffs-their properties, uses, hydrology, and resources. Spec Pap Geol Soc Am 408:1–134. https://doi.org/10.1130/0-8137-2408-2.1

Holik JS, Rabinowitz PD, Austin JA (1991) Effects of Canary hotspot volcanism on structure of oceanic crust off Morocco. J Geophys Res Solid Earth 96:12039–12067. https://doi.org/10.1029/91JB00709

IGME. Instituto Geológico y Minero de España (2021) Continuous geological map of Spain scale 1/50.000. Ministerio de Ciencias e Innovación. Retrieved (http://info.igme.es/visor%20web/)

Ince I, Fener M (2016) A prediction model for uniaxial compressive strength of deteriorated pyroclastic rocks due to freeze–thaw cycle. J African Earth Sci 120:134–140. https://doi.org/10.1016/J.JAFREARSCI.2016.05.001

Isabel M, Borges A (2019) Estudio de la acción de ambientes agresivos en rocas graníticas del Alentejo. https://dehesa.unex.es:8443/handle/10662/9997. Accessed Jan 8, 2022

Iucolano F, Colella A, Liguori B et al (2019) Suitability of silica nanoparticles for tuff consolidation. Constr Build Mater 202:73–81. https://doi.org/10.1016/J.CONBUILDMAT.2019.01.002

Jamshidi A, Nikudel MR, Khamechiyan M (2013a) Estimating the durability of building stones against Salt crystallization: considering the physical properties and strength characteristics. Geopersia 3:35–48. https://doi.org/10.22059/JGEOPE.2013.36013

Jamshidi A, Nikudel MR, Khamehchiyan M (2013b) Predicting the long-term durability of building stones against freeze–thaw using a decay function model. Cold Reg Sci Technol 92:29–36. https://doi.org/10.1016/J.COLDREGIONS.2013.03.007

Kahraman S, Delibalta MS, Comakli R et al (2016) Predicting the noise level in rock sawing from the physico-mechanical and mineralogical properties of rocks. Appl Acoust 114:244–251. https://doi.org/10.1016/J.APACOUST.2016.08.004

Karaca Z, Günes YIlmaz N, Goktan RM (2012) Considerations on the European Standard en 14157 test methods: Abrasion resistance of natural stones used for flooring in buildings. Rock Mech Rock Eng 45:103–111. https://doi.org/10.1007/S00603-011-0190-1/FIGURES/15

Karaca Z, Hamdi Deliormanli A, Elci H, Pamukcu C (2010) Effect of freeze–thaw process on the abrasion loss value of stones. Int J Rock Mech Min Sci 47:1207–1211. https://doi.org/10.1016/J.IJRMMS.2010.07.003

Karakaş A, Morali G, Coruk Ö, Bozkurtoğlu E (2021) Geomechanical, durability–hygrothermal and thermal shock properties of Kocaeli Kandira stone used as building stone in historical structures. Environ Earth Sci 80:1–15. https://doi.org/10.1007/S12665-021-09426-8/TABLES/11

Kekec B, Gokay MK (2009) Mechanical properties of Erciyes mountain volcanics and their usability as dimensional building stone. 9th International Multidisciplinary Scientific Geoconference. In conference proceeding: Modern Management of mine producing, geology and environmental protection. SGEM 14, Bulgaria pp. 441–448

Kılıç A, Teymen A (2008) Determination of mechanical properties of rocks using simple methods. Bull Eng Geol Environ 67:237–244. https://doi.org/10.1007/S10064-008-0128-3/FIGURES/15

Kłopotowska AK, Łukaszewski P (2014) The Influence of the Salt Mist on the Deterioration of Rock Materials. Stud Geotech Mech 36:37–45. https://doi.org/10.2478/SGEM-2014-0005

Kolgitti T, Çelik SB (2022) Investigation of the usability of wide wheel abrasion test on rock core samples. Environ Earth Sci 81:1–15. https://doi.org/10.1007/S12665-022-10661-W/FIGURES/16

Koralay T, Çelik SB (2019) Minero-petrographical, physical, and mechanical properties of moderately welded ignimbrite as a traditional building stone from Uşak Region (SW Turkey). Arab J Geosci 12:1–17. https://doi.org/10.1007/S12517-019-4923-X/TABLES/8

Koralay T, Özkul M, Kumsar H et al (2011) The effect of welding degree on geotechnical properties of an ignimbrite flow unit: The Bitlis castle case (eastern Turkey). Environ Earth Sci 64:869–881. https://doi.org/10.1007/S12665-011-0931-1/FIGURES/10

Korkanç M (2007) The effect of geomechanical properties of ignimbrites on their usage as building stone: Nevşehir stone. Jeol Muhendisligi Derg 31:49–60

Kundak E, Akdaş H, Sariişik G (2020) Farkli kalinliktaki bazi doğal taşlarin kopma enerjisi ve çarpma dayaniminin belirlenmesi. J Eng Archit Fac Eskisehir Osmangazi Univ 28:62–72. https://doi.org/10.31796/OGUMMF.690196

Laskaridis K, Arapakou A, Patronis M et al (2021) Physical mechanical properties and producing areas of greek dimension stones. Mater Proc 5:64. https://doi.org/10.3390/MATERPROC2021005064

Lefèvre RA, Ausset P (2002) Atmospheric pollution and building materials: Stone and glass. Geol Soc Spec Publ 205:329–345. https://doi.org/10.1144/GSL.SP.2002.205.01.24

Lezzerini M, Civita J, Aquino A et al (2021) Marbles from Castagneto Carducci Area (Tuscany, Italy). IOP Conf Ser Earth Environ Sci 906:012122. https://doi.org/10.1088/1755-1315/906/1/012122

López-Doncel R, Wedekind W, Dohrmann R, Siegesmund S (2013) Moisture expansion associated to secondary porosity: An example of the Loseros Tuff of Guanajuato, Mexico. Environ Earth Sci 69:1189–1201. https://doi.org/10.1007/S12665-012-1781-1/FIGURES/13

López-Doncel R, Wedekind W, Leiser T et al (2016) Salt bursting tests on volcanic tuff rocks from Mexico. Environ Earth Sci 75:1–22. https://doi.org/10.1007/S12665-015-4770-3/FIGURES/20

López-Doncel R, Wedekind W, Aguillón-Robles A et al (2018) Thermal expansion on volcanic tuff rocks used as building stones: examples from Mexico. Environ Earth Sci 77:1–23. https://doi.org/10.1007/S12665-018-7533-0/TABLES/10

Machín ARH (2009) Volcanología y geomorfología de la etapa de rejuvenecimiento plio-pleistocena de Gran Canaria (Islas Canarias). University of Las Palmas de Gran Canaria

Marradi A, Secchiari L, Lezzerini M (2008) The qualification of stone materials for their application in road stone pavements. In: Conference: Second International Congress on Dimension Stones. Carrara-Italy.

Marrero-Cabrera JL (2000) Introducción. In: Excmo. Ayuntamiento de Arucas, Fundación para la Etnografía y el Dearrollo de la Artesanía Canria (FEDAC) (eds) Los Labrantes de Arucas. Ediciones del Umbral, Las Palmas de Gran Canaria, pp 24

Martínez-Martínez J, Pola A, García-Sánchez L et al (2018) Building stones used in the architectural heritage of Morelia (México): quarries location, rock durability and stone compatibility in the monument. Environ Earth Sci 77:1–16. https://doi.org/10.1007/S12665-018-7340-7/TABLES/6

McLennan SM (1982) On the geochemical evolution of sedimentary rocks. Chem Geol 37:335–350. https://doi.org/10.1016/0009-2541(82)90087-0

Merico A, Bellopede R, Fiorucci A et al (2022) Itria Valley (Apulia, Italy): Comparison of limestones for the construction and restoration of "Trulli" roofing. Resour Policy 76. https://doi.org/10.1016/J.RESOURPOL.2022.102630

Mokrzycki WS, Tatol M (2011) Colour difference δE - A survey. Mach Graph vis 20:383–411

Molina E, Arizzi A, Benavente D et al (2020) Influence of Surface Finishes and a Calcium Phosphate-Based Consolidant on the Decay of Sedimentary Building Stones Due to Acid Attack. Front Mater 7:360. https://doi.org/10.3389/FMATS.2020.581979/BIBTEX

Mota-López MI, Fort R, Buergo MA et al (2022) Analytical characterisation of the granitic rocks used in the vomitoria of the Roman amphitheatre in Emerita Augusta. Rend Lincei 33:57–70. https://doi.org/10.1007/S12210-022-01058-9/FIGURES/15

Navarro R, Cruz AS, Arriaga L, Baltuille JM (2017) Caracterización de los principales tipos de mármol extraídos en la comarca de Macael (Almería, sureste de España) y su importancia a lo largo de la historia. Bol Geol y Min 128:345–361. https://doi.org/10.21701/BOLGEOMIN.128.2.005

Negredo AM, van Hunen J, Rodríguez-González J, Fullea J (2022) On the origin of the Canary Islands: Insights from mantle convection modelling. Earth Planet Sci Lett 584:117506. https://doi.org/10.1016/J.EPSL.2022.117506

Nesbitt HW, Young GM (1982) Early proterozoic climates and plate motions inferred from major element chemistry of lutites. Nature 299:715–717. https://doi.org/10.1038/299715A0

Oliveira LI (2017) Estudo de um traquito da região de Mafra para aplicação como rocha ornamental. Master's thesis. University of Nova de Lisboa, Lisboa, Portugal.

Öner F, Türkmen S, Özbek A, Karakaya T (2006) Engineering properties of Hınıs ignimbrites and their usability as a building stone (Erzurum, Turkey). Environ Geol 50:275–284. https://doi.org/10.1007/s00254-006-0208-2

Ortega-Díaz F, Aparicio P, Galán E (2014) Limitations of the standard procedure for the evaluation of marble and limestone for use in construction: a critical analysis and proposal for modification. Restor Build Monum 17:309–320. https://doi.org/10.1515/RBM-2011-6468

Özbek A (2014) Investigation of the effects of wetting-drying and freezing-thawing cycles on some physical and mechanical properties of selected ignimbrites. Bull Eng Geol Environ 73:595–609. https://doi.org/10.1007/S10064-013-0519-Y/TABLES/11

Özşen H, Bozdağ A, İnce İ (2017) Effect of salt crystallization on weathering of pyroclastic rocks from Cappadocia, Turkey. Arab J Geosci 10:1–8. https://doi.org/10.1007/S12517-017-3027-8/FIGURES/5

Özvan A, Direk N (2021) The relationships among different abrasion tests on deteriorated and undeteriorated rocks. Bull Eng Geol Environ 80:1745–1756. https://doi.org/10.1007/S10064-020-02041-0/TABLES/7

Perez-Torrado FJ, Carracedo JC, Mangas J (1995) Geochronology and stratigraphy of the Roque Nublo Cycle, Gran Canaria, Canary Islands. J Geol Soc London 152:807–818. https://doi.org/10.1144/GSJGS.152.5.0807

Pötzl C, Dohrmann R, Siegesmund S (2018a) Clay swelling mechanism in tuff stones: an example of the Hilbersdorf Tuff from Chemnitz, Germany. Environ Earth Sci 77:1–19. https://doi.org/10.1007/S12665-018-7345-2/FIGURES/15

Pötzl C, Siegesmund S, Dohrmann R, Koning JM, Wedekind W (2018b) Deterioration of volcanic tuff rocks from Armenia: constraints on salt crystallization and hydric expansion. Environ Earth Sci 77:1–36. https://doi.org/10.1007/S12665-018-7777-8/FIGURES/36

Pötzl C, Siegesmund S, López-Doncel R, Dohrmann R (2022) Key parameters of volcanic tuffs used as building stone: a statistical approach. Environ Earth Sci 81:1–29. https://doi.org/10.1007/S12665-021-10114-W/TABLES/6

Primavori P, Angheben A (2020) Trentino porphyry, Italy. In: Geological Society Special Publication.Vol. 486 Geological Society of London pp. 33–51. https://doi.org/10.1144/SP486-2020-20

Rodríguez-Losada JA, Hernández-Gutiérrez LE, Mora-Figueroa AL (2007) Geotechnical features of the welded ignimbrites of the Canary Islands. In: Volcanic Rocks - Proceedings of the International Workshop on Volcanic Rocks, Workshop W2 - 11th Congress ISRM. pp. 29–33. https://doi.org/10.1201/noe0415451406.ch4

Romero MB, Ullauri MA, Bustamante R et al (2022) The quantification of physico-mechanical properties and durability of onyx-travertines from Santa Ana de los Ríos de Cuenca, Ecuador. Herit Sci 10:1–19. https://doi.org/10.1186/S40494-022-00826-Y/FIGURES/7

Santos I, Sousa L, Lourenço J (2018) Granite resource evaluation: example of an extraction area in the north of Portugal. Environ Earth Sci 77:1–14. https://doi.org/10.1007/S12665-018-7780-0/TABLES/5

Sarıışık G, Özkan E, Kundak E, Akdaş H (2016) Classification of Parameters Affecting Impact Resistance of Natural Stones. J Test Eval 44:20140276. https://doi.org/10.1520/jte20140276

Schiavon N (2007) Kaolinisation of granite in an urban environment. Environ Geol 52:333–341. https://doi.org/10.1007/S00254-006-0473-0

Schirnick C, den Bogaard P, Schmincke HU (1999) Cone sheet formation and intrusive growth of an oceanic island---The Miocene Tejeda complex on Gran Canaria (Canary Islands). Geology 27. https://doi.org/10.1130/0091-7613(1999)027<0207:CSFAIG>2.3.CO;2

Schmincke HU (1967) Cone sheet swarm, resurgence of tejeda caldera, and the early geologic history of gran Canaria. Bull Volcanol 31:153–162. https://doi.org/10.1007/BF02597011/METRICS

Schmincke HU, Sumita M (1998) Volcanic evolution of Gran Canaria reconstructed from apron sediments: Synthesis of Vicap Project drilling. Proc Ocean Drill Progr Sci Results 157:443–469. https://doi.org/10.2973/ODP.PROC.SR.157.135.1998

Schmincke HU (1990) Geological field guide, Gran Canaria. IAVCEI. In: International Volcanological Congress IAVCEI. Mainz pp. 2–209.

Schmincke HU (1993) Geological field guide of Gran Canaria. ARRAY(0x557cec3205f0): Witten https://oceanrep.geomar.de/id/eprint/35737/

Selby JM (1980) A rock mass strength classification for geomorphic purposes: with tests from Antarctica and New Zealand. Zeitschrift Für Geomorphol 24:31–51. https://doi.org/10.1127/ZFG/24/1984/31

Selim HH, Karakaş A, Coruk Ö (2019) Investigation of engineering properties for usability of Lefke stone (Osmaneli/Bilecik) as building stone. Bull Eng Geol Environ 78:6047–6059. https://doi.org/10.1007/S10064-019-01520-3/FIGURES/8

Fonseca BMS (2012) Influência do nevoeiro salino na degradação de materiais cerâmicos aplicados em construções. Faculdade de Ciências e Tecnologia https://run.unl.pt/handle/10362/7558. Accessed 11 Mar 2023

Sert M, Özkahraman HT (2016) The importance of welded tuff stones in building construction according to their physico-mechanical properties. Harran Univ J Eng 1:8–18. https://dergipark.org.tr/en/pub/humder/issue/28975/309939. Accessed 28 Feb 2023

Shao J, Yang S, Li C (2012) Chemical indices (CIA and WIP) as proxies for integrated chemical weathering in China: Inferences from analysis of fluvial sediments. Sediment Geol 265–266:110–120. https://doi.org/10.1016/J.SEDGEO.2012.03.020

Siedel H, Rust M, Goth K, Krüger A, Heidenfelder W (2019) Rochlitz porphyry tuff ("Rochlitzer Porphyrtuff"): A candidate for "Global Heritage Stone Resource" designation from Germany. Episodes J Int Geosci 42:81–91. https://doi.org/10.18814/EPIIUGS/2019/019007

Siegesmund S, Sousa L, López-Doncel R (2018) Editorial to the topical collection in Environmental Earth Sciences "Stone in the architectural heritage: from quarry to monuments—environment, exploitation, properties and durability." Environ Earth Sci 77:1–4. https://doi.org/10.1007/S12665-018-7755-1/METRICS

Siegesmund S, Pötzl C, López-Doncel R et al (2022) Overview and quality assessment of volcanic tuffs in the Mexican building heritage. Environ Earth Sci 81:1–37. https://doi.org/10.1007/S12665-022-10530-6/FIGURES/13

Silva JBP, Carvalho C, Caetano SD, Gomes C (2010) Natural stone from the Azores archipelago: Relationship between lithology and physical-mechanical behaviour. In: ISRM International Workshop on Rock Mechanics and Geoengineering in Volcanic Environments 2010, IWVE 2010. International Society for Rock Mechanics pp. 125–131.

Simão J, Carvalho C, Silva Z, Moura A, Associado com Agregação P (2010) Factor de qualidade em rochas ornamentais com base em ensaios mecânicos e envelhecimento artificial. Geotecnia. http://repositorio.lneg.pt/handle/10400.9/2712. Accessed 7 Jan 2022

Simão J, Leal N, Gartmann, Silva Z (2011) Salt-fog experiments on consolidant and water-repellent treated dimension stones.

Simão J, Pires V, Galhano C (2015) Salt fog experiments on natural stone. The case of three Portuguese ornamental limestones. In: International Conference on Engineering (ICEUBI2015).

Snethlage R (2005) Methoden und Laboruntersuchungen zur Konservierung. In: Leitfaden Steinkonservierung: Planung von Untersuchungen und Maßnahmen zur Erhaltung von Denkmälern aus Naturstein. Stuttgart. Verlag, Raunhofer I, editor. Vol. 289 Leitfaden Steinkonservierung pp. 109–192.

Socorro JS, Carracedo JC, Pérez-Torrado FJ, Hansen A (2005) *Canarias, volcanes en el mar II. Historia del volcán de Tejeda*. Servicio de Publicaciones de la Caja General de Ahorros de Canarias: Tenerife

Sousa L, Lourenço J, Pereira D (2019) Suitable Re-Use of Abandoned Quarries for Restoration and Conservation of the Old City of Salamanca—World Heritage Site. Sustain 11:4352. https://doi.org/10.3390/SU11164352

Sousa L (2014) Petrophysical properties and durability of granites employed as building stone: a comprehensive evaluation. Bull Eng Geol Environ 73:569–588. https://doi.org/10.1007/S10064-013-0553-9

Sousa LMO, Suárez del Río LM, Calleja L, Ruiz de Argandoña VG, Rodríguez Rey A (2005) Influence of microfractures and porosity on the physico-mechanical properties and weathering of ornamental granites. Eng Geol 77:153–168. https://doi.org/10.1016/J.ENGGEO.2004.10.001

Sousa L, Oliveira AS, Alves IMC (2016) Influence of fracture system on the exploitation of building stones: the case of the Mondim de Basto granite (north Portugal). Environ Earth Sci 75:1–16. https://doi.org/10.1007/S12665-015-4824-6/FIGURES/16

Sousa L, Menningen J, López-Doncel R, Siegesmund S (2021) Petrophysical properties of limestones: influence on behaviour under different environmental conditions and applications. Environ Earth Sci 80:1–19. https://doi.org/10.1007/S12665-021-10064-3/FIGURES/9

Spathis PK, Mavrommati M, Gkrava E et al (2021) Characterization of natural stone from the archaeological site of pella, Macedonia, Northern Greece. Heritage 4:4665–4677. https://doi.org/10.3390/HERITAGE4040257

Sreejith C, Del Lama EA, Kaur G (2021) Charnockite: a candidate for 'Global Heritage Stone Resource'' designation from India'. Episodes J Int Geosci 44:19–29. https://doi.org/10.18814/EPIIUGS/2020/0200S11

Seymour K et al. (2004) Romancing the stone: construction of monuments & works of art from volcanic rock. In: Proceedings of the 7th pan-hellenic geographical conference of the Hellenic Geographical Association, Mytilene, Lesvos, Greece, pp 14–17

Stück H, Forgó LZ, Rüdrich J et al (2008) The behaviour of consolidated volcanic tuffs: Weathering mechanisms under simulated laboratory conditions. Environ Geol 56:699–713. https://doi.org/10.1007/S00254-008-1337-6/FIGURES/7

Tel HÖ, Sarıışık G (2020) Research on some effective properties in nomination of Urfa Limestone to the "Global Heritage Stone Resource" designation. Arab J Geosci 13:1–15. https://doi.org/10.1007/S12517-020-05948-W/FIGURES/13

Teymen A (2018) Prediction of basic mechanical properties of tuffs using physical and index tests. J Min Sci 545(54):721–733. https://doi.org/10.1134/S1062739118054820

Teymen A, Mengüç EC (2020) Comparative evaluation of different statistical tools for the prediction of uniaxial compressive strength of rocks. Int J Min Sci Technol 30:785–797. https://doi.org/10.1016/J.IJMST.2020.06.008

Topal T, Sözmen B (2001) Characteristics of the Weathering Zones Developed Within the Tuffs of the Midas Monument. Turkish J Earth Sci 10:83–91.

Toprak MU, Arslanbaba MA (2016) Possibility of using Kütahya Volcanic Tuff as building stone: Microstructural evaluation and strength enhancement through heat treatment. Constr Build Mater 110:128–134. https://doi.org/10.1016/J.CONBUILDMAT.2016.02.024

Troll VR, Walter TR, Schmincke H-U (2002) Cyclic caldera collapse: Piston or piecemeal subsidence? Field and experimental evidence. Geology 30:135–138. https://doi.org/10.1130/0091-7613(2002)030%3c0135:CCCPOP%3e2.0.CO;2

Türkdönmez O, Bozcu M (2012) The Geological, Petrographical and Engineering Properties of Rhyolitic Tuffs (Çan Stone) in Çan-Etili Area (Çanakkale), NW Turkey: Their Usage as Building and Covering Stones. Open J Geol 2:25–33. https://doi.org/10.4236/OJG.2012.21003

Ünal M, Altunok E (2019) Determination of water absorption properties of natural building stones and their relation to porosity.

E-journal New World Sci Acad 14:39–45. https://doi.org/10.12739/NWSA.2019.14.1.1A0429

Ünal M (2011) The effect of salt crystallization on Tuff used as building material. Eng Sci 6:41–49. https://doi.org/10.12739/NWSAES.V6I1.5000067005

UNE-EN 12370:1999. Natural stone test methods. Determination of resistance to salt crystallisation. AENOR (Spanish Association for Standardisation and Certification)

Valido JA, Laz MM, Cáceres JM (2021) Lithology, physical and mechanical characterization of Chinese Porphyry. IOP Conf Ser Earth Environ Sci 833:012029. https://doi.org/10.1088/1755-1315/833/1/012029

Valido JA, Cáceres JM, Sousa L (2023) A characterisation study of ignimbrites of Tenerife Island employed as building stone. Environ Earth Sci 82:280. https://doi.org/10.21203/rs.3.rs-2521070/v1

Van Den Bogaard P (2013) The origin of the Canary Island Seamount Province - New ages of old seamounts. Sci Reports 3:2107. https://doi.org/10.1038/srep02107

Van den Bogaard P, Schmincke HU (1998) Chronostratigraphy of Gran Canaria. Proc Ocean Drill Progr Sci Results 157:127–140. https://doi.org/10.2973/ODP.PROC.SR.157.116.1998

Vanorio T, Prasad M, Patella D, Nur A (2002) Ultrasonic velocity measurements in volcanic rocks: correlation with microtexture. Geophys J Int 149:22–36. https://doi.org/10.1046/J.0956-540X.2001.01580.X

Vavro M, Vavro L, Martinec P, Souček K (2016) Properties, durability and use of glauconitic Godula sandstones: a relatively less known building stone of the Czech Republic and Poland. Environ Earth Sci 75:1–17. https://doi.org/10.1007/S12665-016-6248-3/TABLES/5

Warr LN (2021) IMA–CNMNC approved mineral symbols. Mineral Mag 85:291–320. https://doi.org/10.1180/mgm.2021.43

Wedekind W, Ruedrich J, Siegesmund S (2011) Natural building stones of Mexico-Tenochtitlán: Their use, weathering and rock properties at the Templo Mayor, Palace Heras Soto and the Metropolitan Cathedral. Environ Earth Sci 63:1787–1798. https://doi.org/10.1007/S12665-011-1075-Z/TABLES/4

Wedekind W, López-Doncel R, Dohrmann R, Kocher M, Siegesmund S (2013) Weathering of volcanic tuff rocks caused by moisture expansion. Environ Earth Sci 69:1203–1224. https://doi.org/10.1007/S12665-012-2158-1/FIGURES/19

Yarahmadi R, Bagherpour R, Khademian A et al (2019) Determining the optimum cutting direction in granite quarries through experimental studies: a case study of a granite quarry. Bull Eng Geol Environ 78:459–467. https://doi.org/10.1007/S10064-017-1158-5

Yavuz AB (2012) Durability assessment of the Alaçatı tuff (Izmir) in western Turkey. Environ Earth Sci 67:1909–1925. https://doi.org/10.1007/S12665-012-1632-0/FIGURES/13

Yavuz AB, Akal C, Türk N, Çolak M, Tanyu BF (2015) Investigation of discrepancy between tuff used as building stones in historical and modern buildings in western Turkey. Constr Build Mater 93:439–448. https://doi.org/10.1016/J.CONBUILDMAT.2015.06.017

Yüksek S (2019) Mechanical properties of some building stones from volcanic deposits of mount Erciyes (Turkey). Mater Construcción 69:187. https://doi.org/10.3989/mc.2019.04618

Yüksek S, Demirci A (2010) Geotechnical properties of volcanic materials of the Mount Erciyes. In: ISRM international workshop on rock mechanics and geoengineering in volcanic environments 2010, IWVE 2010. International Society for Rock Mechanics, pp 99–105. https://doi.org/10.1201/b10549-15